Major ginsenosides from Panax ginseng promote aerobic cellular respiration and SIRT1-mediated mitochondrial biosynthesis in cardiomyocytes and neurons

Qingxia Huang[1], Tingting Lou[1], Jing Lu[2], Manying Wang[2], Xuenan Chen[2], Linyuan Xue[2], Xiaolei Tang[2], Wenxiu Qi[1], Zepeng Zhang[2], Hang Su[1], Wenqi Jin[2], Chenxu Jing[2], Daqing Zhao[1], Liwei Sun[2], and Xiangyan Li[1]

[1]Changchun University of Chinese Medicine
[2]First Affiliated Hospital to Changchun University of Chinese Medicine

March 30, 2022

Abstract

Aerobic cellular respiration provides chemical energy, adenosine triphosphate (ATP), to maintain multiple cellular functions. Sirtuin 1 (SIRT1) can deacetylate peroxisome proliferator-activated receptor gamma coactivator 1 alpha (PGC-1α) to promote mitochondrial biosynthesis. Targeting energy metabolism is a potential strategy for the prevention and treatment of various diseases, such as cardiac and neurological disorders. Ginsenosides, one of the major bioactive constituents of Panax ginseng, have been extensively used due to their diverse beneficial effects on healthy subjects and patients with different diseases. However, the underlying molecular mechanisms of total ginsenosides (GS) on energy metabolism remain unclear. In this study, oxygen consumption rate, ATP production, mitochondrial biosynthesis, glucose metabolism, and SIRT1-PGC-1α pathways in untreated and GS-treated different cells, fly, and mouse models were investigated. GS pretreatment enhanced mitochondrial respiration capacity and ATP production in aerobic respiration-dominated cardiomyocytes and neurons, and promoted tricarboxylic acid metabolism in cardiomyocytes. Moreover, GS clearly enhanced NAD+-dependent SIRT1 activation to increase mitochondrial biosynthesis in cardiomyocytes and neurons, which was completely abrogated by nicotinamide. In addition, GS had protective effects against hypoxia- or oxygen-glucose deprivation-induced cardiomyocyte damage through activation of the SIRT1-PGC-1α pathway. Importantly, ginsenoside monomers, such as Rg1, Re, Rf, Rb1, Rc, Rh1, Rb2, and Rb3, were found to activate SIRT1 and promote energy metabolism. This study may provide new insights into the extensive application of ginseng for cardiac and neurological protection in healthy subjects and patients with ischemic disorders.

Major ginsenosides from*Panax ginseng* promote aerobic cellular respiration and SIRT1-mediated mitochondrial biosynthesis in cardiomyocytes and neurons

Short title: Major ginsenosides promotes mitochondrial function

Qingxia Huang[1,2], Tingting Lou[2], Jing Lu[2], Manying Wang[2], Xuenan Chen[2], Linyuan Xue[2], Xiaolei Tang[2], Wenxiu Qi[1], Zepeng Zhang[2], Hang Su[3], Wenqi Jin[2], Chenxu Jing[2], Daqing Zhao[1*], Liwei Sun[2*], Xiangyan Li[1*]

[1]Jilin Ginseng Academy, Key Laboratory of Active Substances and Biological Mechanisms of Ginseng Efficacy, Ministry of Education, Jilin Provincial Key Laboratory of Bio-Macromolecules of Chinese Medicine, Changchun University of Chinese Medicine, Changchun, Jilin, China

[2]Research Center of Traditional Chinese Medicine, the First Affiliated Hospital to Changchun University of Chinese Medicine, Changchun, Jilin, China

[3]Practice Innovations Center, Changchun University of Chinese Medicine, Changchun, Jilin, China

*Corresponding authors:

Daqing Zhao, Xiangyan Li: Jilin Ginseng Academy, Key Laboratory of Active Substances and Biological Mechanisms of Ginseng Efficacy, Ministry of Education, Jilin Provincial Key Laboratory of BioMacromolecules of Chinese Medicine, Changchun University of Chinese Medicine, Changchun, Jilin, China.

Liwei Sun: Research Center of Traditional Chinese Medicine, First Affiliated Hospital to Changchun University of Chinese Medicine, Changchun, Jilin, China. Tel.: +86-431-86177630, Fax: +86-431-86177630. Email: zhaodaqing1963@163.com; sunnylilwei@163.com; xiangyan_li1981@163.com.

Acknowledgments:

We thank you for the kind supports on mouse model from Shuang Liu and Guan Wang, College of Life Science, Jilin University. We appreciate the comments for data organization from Tong Li, School of Medicine, Johns Hopkins University.

Conflict of interest statement:

All authors declare that they have no conflict of interest.

Abstract

Background and Purpose : Aerobic cellular respiration provides chemical energy, adenosine triphosphate (ATP), to maintain multiple cellular functions. Sirtuin 1 (SIRT1) can deacetylate peroxisome proliferator-activated receptor gamma coactivator 1 alpha (PGC-1α) to promote mitochondrial biosynthesis. Targeting energy metabolism is a potential strategy for the prevention and treatment of various diseases, such as cardiac and neurological disorders. Ginsenosides, one of the major bioactive constituents of *Panax* ginseng, have been extensively used due to their diverse beneficial effects on healthy subjects and patients with different diseases. However, the underlying molecular mechanisms of total ginsenosides (GS) on energy metabolism remain unclear. *Experimental Approach* : In this study, oxygen consumption rate, ATP production, mitochondrial biosynthesis, glucose metabolism, and SIRT1-PGC-1α pathways in untreated and GS-treated different cells, fly, and mouse models were investigated. *Key Results* : GS pretreatment enhanced mitochondrial respiration capacity and ATP production in aerobic respiration-dominated cardiomyocytes and neurons, and promoted tricarboxylic acid metabolism in cardiomyocytes. Moreover, GS clearly enhanced NAD^+-dependent SIRT1 activation to increase mitochondrial biosynthesis in cardiomyocytes and neurons, which was completely abrogated by nicotinamide. In addition, GS had protective effects against hypoxia- or oxygen-glucose deprivation-induced cardiomyocyte damage through activation of the SIRT1-PGC-1α pathway. Importantly, ginsenoside monomers, such as Rg1, Re, Rf, Rb1, Rc, Rh1, Rb2, and Rb3, were found to activate SIRT1 and promote energy metabolism. *Conclusion and Implications* : GS promotes aerobic cellular respiration and SIRT1-mediated mitochondrial biosynthesis, which may provide new insights into the extensive application of ginseng for cardiac and neurological protection in healthy subjects and patients with ischemic disorders.

Key Words : ginsenosides, aerobic cellular respiration, mitochondrial biosynthesis, SIRT1, PGC1α, cardiomyocytes, neurons

Abbreviations:

ATP adenosine triphosphate

HK-I/II hexokinase I/II

PFK-1 phosphofructokinase-1

PK pyruvate kinase

MPC mitochondrial pyruvate carrier

PDH pyruvate dehydrogenase

TCA tricarboxylic acid

NADH nicotinamide adenine dinucleotide

FADH2 flavin adenine dinucleotide

ETC electron transport chain

OGD oxygen-glucose deprivation

NAD^+ Oxidized nicotinamide adenine dinucleotide

SIRT1 sirtuin 1

PGC-1α peroxisome proliferator initiated receptor gamma and coactivator 1 alpha

Nrf-1 nuclear respiratory factor-1

I/R ischemia/reperfusion

GS total ginsenosides

OCR oxygen consumption rate

MRC mitochondrial respiration capacity

CS citrate synthase

IDH1/2 isocitrate dehydrogenase 1/2

DLST dihydrolipoamide S-succinyltransferase

SDHA succinate dehydrogenase complex, subunit A

ACO2 aconitase 2

GAPDH glyceraldehyde-3-phosphate dehydrogenase

PDH pyruvate dehydrogenase

PFKP platelet-type phosphofructokinase

HPLC high-performance liquid chromatography

NAM Nicotinamide

LC-MS liquid chromatography-mass spectrometry

BMSCs bone marrow mesenchymal stem cells

HUVECs human umbilical vein endothelial cells

qPCR Quantitative PCR

Bullet points:

What is already known: Ginsenosides, one of the major bioactive constituents of *Panax* ginseng, have been extensively used due to their diverse beneficial effects on healthy subjects and patients with different diseases.

What this study adds: Total ginsenosides enhances mitochondrial respiration capacity, ATP production and promotes NAD^+-dependent SIRT1 activation to increase mitochondrial biosynthesis in cardiomyocytes and neurons. Rg1, Re, Rf, Rb1, Rc, Rh1, Rb2, and Rb3 are major ginsenoside monomers for SIRT1 activation and enhanced energy metabolism.

Clinical significance: This study may provide new insights into the extensive application of ginseng for cardiac and neurological protection in healthy subjects and patients with ischemic disorders.

Introduction

Aerobic cellular respiration refers to the process by which organisms convert nutrients into chemical energy, adenosine triphosphate (ATP), using oxygen, which is dominated in highly aerobic tissues, such as cardiac and neural systems (Hall, Klein-Flugge, Howarth & Attwell, 2012; Hickey et al., 2009; Neubauer, 2007). During glucose aerobic metabolism, glucose with 6-carbon is broken down into 3-carbon pyruvate by multiple key enzymes such as hexokinase-I/II (HK-I/II), phosphofructokinase-1 (PFK-1), and pyruvate kinase (PK) in the cytoplasm. Then pyruvate is transported into the mitochondria through the mitochondrial pyruvate carrier (MPC) (Bricker et al., 2012) and metabolized to synthesize acetyl-coenzyme A (CoA) by pyruvate dehydrogenase (PDH) (Sugden & Holness, 2003). After the metabolism of tricarboxylic acid (TCA) cycle, nicotinamide adenine dinucleotide (NADH) and flavin adenine dinucleotide (FADH2) from acetyl-CoA can pass their electrons into the mitochondrial electron transport chain (ETC) to produce ATP molecules, with the help of oxygen (Fernie, Carrari & Sweetlove, 2004). During this process, respiratory chain protein complexes I-V embedded in the inner mitochondrial membrane is involved in ATP production (Wallace, Fan & Procaccio, 2010). Abnormal energy metabolism is a critical target during the progression of disease, including myocardial ischemia, heart failure (Fillmore & Lopaschuk, 2013), stoke (Narne, Pandey & Phanithi, 2017), or neurodegenerative diseases (Butterfield & Halliwell, 2019). During the exposure to hypoxia, cells display decreased carbon flux into the TCA cycle and diminished electron flux through ETC (Papandreou, Cairns, Fontana, Lim & Denko, 2006; Wheaton & Chandel, 2011). Moreover, oxygen-glucose deprivation (OGD) can cause mitochondrial damage and ATP depletion in cardiomyocytes and neurons (Almeida, Delgado-Esteban, Bolanos & Medina, 2002; Kalogeris, Baines, Krenz & Korthuis, 2012). Therefore, the enhancements of glucose oxidation and mitochondrial bioenergy have been potential strategies against various disorders, such as ischemic conditions.

Oxidized nicotinamide adenine dinucleotide (NAD^+) is a well-known small molecule that drives energy metabolism through its electron transfer function (Hopp, Gruter & Hottiger, 2019). Increased NAD^+ level promotes the activity of sirtuin 1 (SIRT1), a strong deacetylase of class III histone deacetylase, which heavily implicates in a number of physical and pathological processes, such as aging-related diseases (Imai & Guarente, 2014). SIRT1 deacetylates its substrate, peroxisome proliferator initiated receptor gamma and coactivator 1 alpha (PGC-1α), to regulate mitochondrial biosynthesis and energy metabolism (Aquilano, Baldelli, Pagliei & Ciriolo, 2013). PGC-1α can bind and co-activate different transcription factors, such as nuclear respiratory factor-1 (Nrf-1) and Nrf-2, in the promoter of mitochondrial transcription factor A (TFAM), which increases the transcription of key mitochondrial enzymes, such as cytochrome c oxidase subunits (COXII, COXIV) and ATP synthase β subunit, and drives mitochondrial DNA transcription and replication through the interaction of TFAM (Irrcher, Adhihetty, Sheehan, Joseph & Hood, 2003; Wu et al., 1999). Previous studies have shown that the activation of SIRT1-PGC-1α pathway plays a protective role in hypoxia or OGD-induced injuries (Ma et al., 2017; Zhou, Wang, Li, Yu & Zhao, 2017), which improves mitochondrial function to prevent and treat ischemic heart or brain disorders (Yang, Mukda & Chen, 2018; Zhao et al., 2019).

Ginsenosides are major active components of *Panax ginseng C.A. Meyer* , a medicinal herb as new-resource health food approved by the Ministry of Health, China. They are extensively used for diverse beneficial effects on myocardial infarction, stroke, and ischemia/reperfusion (I/R) injury (Aravinthan et al., 2015; Jia, Zhang, Huang & Leung, 2012; Liu, Anderson, Fernandez & Dore, 2019). Currently, about 250 ginsenosides have been isolated and identified, which are mainly divided into three groups, protopanaxadiol (PPD, such as Rb1, Rb2, Rc, Rd, Rg3), protopanaxatriol (PPT, such as Re, Rf, Rg1, Rh1), and oleanolic acid (OA, such as Ro), based on their chemical structures (Wu, Kwaku, Li, Yang, Ge & Xu, 2019). Proteomic analysis has shown that total ginsenosides (GS) can increase the expression of proteins in the TCA cycle to enhance cardiac energy metabolism in the ischemic rat (Wang, Zhou, Yi, Jiang & Liu, 2012). Meanwhile, ginsenoside Rb1, Rb3, Rg3, Rg1, Rg5, and compound K exert cardioprotective and neuroprotective effects

by increasing energy metabolism (Chen et al., 2019b; Xu, Ma, Fan, Chen, Zhang & Tang, 2019; Yang et al., 2017), improving mitochondrial dynamics and quality (Dong et al., 2016; Sun et al., 2013), or inhibiting mitochondrial apoptosis (Huang et al., 2020; Li et al., 2018). Importantly, several ginsenosides, such as Rb1, Rc, F1, Rg3, Rh2, and their metabolites M1-M4 have been identified as SIRT1 activators (Ma, Zhou & Yang, 2015; Wang, Liang, Chen & Zhao, 2016; Yang, Ma, Zhou, Xu & Zhang, 2017), which play protective effects on a series of pathological injuries, such as oxidative stress, inflammation, senescence, hypoxia, or OGD (Cheng et al., 2019; Song et al., 2014; Wang et al., 2019). However, the molecular mechanism underlying the effects of GS and each ginsenoside monomer on mitochondrial aerobic metabolism and biosynthesis in cardiomyocytes and neurons remains unclear and needs to be further investigated.

In this study, we first investigated the effect of GS on mitochondrial oxygen consumption rate (OCR) in a series of cell lines, including aerobic respiration-dominated cardiomyocytes, neuronal cells, and skeletal myoblasts (Di Lisa, Canton, Menabo, Kaludercic & Bernardi, 2007; Zeiger, Stankowski & McLaughlin, 2011), as well as anaerobic respiration-dominated vascular endothelial, epithelial, and stem cells (De Bock et al., 2013; Tang et al., 2016). Then ATP production and mitochondrial respiration capacity (MRC) were examined in untreated and GS-treated cardiomyocytes and neurons. Targeted metabolomics and Western blot analysis were performed to observe the effect of GS on the contents of major metabolites and the levels of key multiple enzymes from glycolysis and TCA cycle. Furthermore, NAD^+ level, SIRT1-PGC-1α pathway, and mitochondrial biosynthesis in the cell, Drosophila melanogaster, and mice models were further evaluated to explore the molecular mechanism of GS. In addition, we observed the effect of GS on SIRT1-mediated mitochondrial function in hypoxia- and OGD-induced cell models. Of note, the ginsenoside monomer in GS for promoting SIRT1 activation and mitochondrial energy production was preliminarily identified in cardiomyocytes. This is the first study to explore the molecular mechanism by which GS promote mitochondrial energy metabolism, which may provide new insights into the clinical application of ginseng for the prevention and treatment of cardiac and neurological disorders.

Materials and Methods

Materials and reagents

Total ginsenosides (GS, purity [?] 80%) and ginsenoside monomers (purity [?] 98%), such as Rg1, Re, Rf, Rb1, Rc, Rh1, Rb2, Rb3, Rd, F1, F3, Rk3, S-Rg3, R-Rg3, PPT, Rk1, Rg5, and Rh2, were purchased from Shanghai Yuanye Bio-Technology (Shanghai, China). Carbonyl cyanide 4-(trifluoromethoxy) phenylhydrazone (FCCP, C2920), and rotenone (R8875) were purchased from Sigma-Aldrich (St. Louis, MO, USA). Oligomycin B (ab143424); antimycin (ab141904); antibodies against oxdiative phosphorylation (OXPHOS, ab110413; CV-ATP5A, CIII-UQCRC2, CIV-MTCO1, CII-SDHB, and CI-NDUFB8); SIRT1 (ab189494); PGC-1α (ab54481); Nrf-1 (ab175932); and Nrf-2 (ab137550) were obtained from Abcam (Cambridge, MA, USA). Glycolysis Antibody Sampler Kit (#8337) containing antibodies against HK-I/II, PKM1/2, glyceraldehyde-3-phosphate dehydrogenase (GAPDH), PDH, lactate dehydrogenase isozyme A, and platelet-type phosphofructokinase (PFKP), and Tricarboxylic Acid Cycle Antibody Sampler Kit (#47767) containing antibodies against citrate synthase (CS), isocitrate dehydrogenase 1/2 (IDH1/2), MPC1/2, dihydrolipoamide S-succinyltransferase (DLST), succinate dehydrogenase complex, subunit A (SDHA), aconitase 2 (ACO2), fumarase, and β-Actin (#3700) were purchased from Cell Signaling Technology (Beverly, MA, USA). p2E2 (Q86LE9) and JLA20 (P68139) were obtained from Developmental Studies Hybridoma Bank (Iowa City, IA, USA). Nicotinamide (NAM, HY-B0150) was purchased from MedChemExpress (Shanghai, China).

High-performance liquid chromatography and liquid chromatography-mass spectrometry analysis

The ginsenoside composition of the GS sample was analyzed by high-performance liquid chromatography (HPLC; Agilent Technologies, Billerica, MA, USA) with a diode-array detector (Ultimate3000, DIONEX, Sunnyvale, CA, USA) using the Elite Kromasil C18 column (4.6×250 mm, 5 μm). The mobile phase condition was ultrapure water (solvent A) and acetonitrile (solvent B; Sigma-Aldrich), and the column temperature was set at 35°C. The flow rate was 1.0 mL/min, and the chromatograms were obtained using a UV/VIS

detector at 203 nm. According to the retention time and chromatographic peak area of ginsenoside standards, 18 ginsenosides were identified and quantified as Rg1 (11.23%), Re (18.32%), Rf (4.37%), Rb1 (5.96%), Rc (10.34%), Rh1 (1.40%), Rb2 (3.15%), Rb3 (0.57%), F1 (0.22%), Rd (7.42%), F3 (2.83%), Rk3 (6.30%), S-Rg3 (2.46%), R-Rg3 (1.00%), PPT (0.16%), Rk1 (1.72%), Rg5 (2.31%), and Rh2 (1.68%) in the GS sample**(Supplementary Fig. 1A and 1B)** . Based on mobile phase and elution gradient from HPLC, LC-mass spectrometry (LC-MS) was performed on the Thermo LTQ XL system (Thermo Fisher Scientific, Carlsbad, CA, USA) with the Agilent ZORBAX SB-C18 column (2.1×100 mm, 1.7 μm) to obtain the chromatogram of different ginsenosides in the negative ion mode. MS analysis conditions were set as follows: gas temperature 270 °C, electric voltage 3.5 kV and scan range from 165 to 2000 *m/z*. The MS chromatogram and properties of different ginsenosides from GS are shown in **Supplementary Fig. 2A and 2B** .

Animal and drug administration

Pregnant (16-day-old), neonatal (3-day-old), or 4-week-old Sprague Dawley rats were purchased from the Jilin University Experimental Animal Center (Changchun, China), which were used for the isolation of primary cells such as cardiomyocytes, cortical neurons, or bone marrow mesenchymal stem cells (BMSCs). Five-week-old Kunming mice were purchased from Liaoning Changsheng Biotechnology Co., Ltd (Benxi, China). All animal procedures were performed in accordance with the guidelines approved by the Animal Ethics Committee of Changchun University of Chinese Medicine. After acclimatization under temperature of 23-25°C and 60%-70% humidity with 12 h-day/night cycle, the mice were randomly divided into two groups as control (sterilized distilled water) and GS (100 mg/kg), which were orally administered every day for 3 weeks. General health, food/water intake, and body weight of all mice with free access to food and water were monitored and recorded every day. At the end of the experiment, mice were euthanatized to collect brain and heart tissues for further analysis.

Cell culture

H9c2 rat cardiomyocyte, PC12 rat adrenal pheochromocytoma, L6/C2C12 rat/mouse skeletal muscle myoblast, human umbilical vein endothelial cells (HUVECs), THP-1 human acute monocytic leukemia cell lines were purchased from the American Type Culture Collection (Manassas, VA, USA). The 16-HBE human bronchial epithelial cell line was kindly provided by Procell Life Science & Technology Co., Ltd. (Wuhan, China). Primary neonatal rat cardiomyocytes, cortical neurons, or BMSCs were isolated, established, and identified as our previous protocols (Huang et al., 2018; Jin et al., 2020; Louch, Sheehan & Wolska, 2011). BMSCs were kept in medium with 10 mM β-glycerophosphate, 50 μg/mL ascorbate, and 100 nM dexamethasone for 14 days to differentiate into the osteoblasts (Jin et al., 2020). All cells were cultured in appropriate medium containing 10% fetal bovine serum (CLARK Bioscience, Claymont, DE, USA) and 1% penicillin-streptomycin (Biosharp, Hefei, China) and incubated at 37°C in a water-saturated atmosphere of 5% CO_2. All cell lines tested negative for mycoplasma contamination. Detailed information for cell culture is described in **Supplementary Table 1** .

OCR assay

As previously reported, OCR was measured using the MitoXpress® Xtra probe or Cell Mito Stress Test Kit (Agilent Technologies) by a time-resolved fluorescence (TR-F) plate reader (Cytation 5; BioTek, Winooski, VT, USA) or Seahorse XFp analyzer (Agilent Technologies), respectively (Yepez et al., 2018). After incubation with GS or ginsenoside monomer for 48 h, each well was equilibrated in a CO_2-free incubator at 37°C for 1 h and measured every 2 min over 2 h to obtain TR-F intensity for calculating the initial slopes (μs min^{-1}), according to the phosphorescence lifetime (τ) values. To further analyze mitochondrial respiration, oligomycin (1 μM), FCCP (5 μM), rotenone (Rot, 1 μM), and antimycin A (AA, 1 μM) were sequentially added to each well with XF base medium (Agilent, pH 7.4) supplemented with 2 mM L-glutamine, 1 mM pyruvate, and 25 mM glucose. After normalization to the intensity of Hoechst 33342 nuclear staining, basal OCR, ATP production, maximal respiratory capacity (MRC), and spare respiratory capacity (SRC) were calculated.

Metabolite measurements

Major intermediates for glycolysis, TCA cycle, and oxidative-phosphorylation were analyzed with the assistance of Applied Protein Technology Co., Ltd. (Shanghai, China), as previously described (Mitsuishi et al., 2012). Briefly, 10 samples of untreated and treated cells (H9c2 and HUVECs) were stored in liquid nitrogen and centrifuged at 14,000 rpm for 20 min to collect the supernatants, which were dried by vacuum. Then, cold acetonitrile/H_2O (1:1, v/v) was added to each sample and centrifuged at 14,000 rpm for 20 min to obtain the supernatants, which were separated and analyzed using a UHPLC (1290 Infinity LC system; Agilent Technologies) coupled to the Triple Quad 5500 Mass Spectrometer (QTRAP/MS; AB SCIEX, Framingham, MA, USA). The raw MS data were processed using Multiquant software based on chromatographic peak area and retention time to identify different energy metabolism-related metabolites.

Measurement of PDH activity

PDH activity was measured using a commercial assay kit (ab109902; Abcam), according to the manufacturer's instruction (Baccelli et al., 2019). Briefly, cell lysates from different groups were loaded onto the 96-well plates coated with an anti-PDH monoclonal antibody and incubated for 3 h at room temperature for the measurement of optical density at 450 nm (OD 450 nm) for 30 min with 1 min internal in a kinetic mode. The relative PDH activity was calculated as the rate (mOD/min) = (absorbance 2-absorbance 1)/time (min).

Quantification of ATP and NAD/NADH levels

According to the manufacturer's instructions, the contents of ATP, NAD^+, and NADH in the cells of different groups were detected using the ATP Assay System Bioluminescence Detection Kit (FF2000; Promega, Madison, WI, USA) and NAD/NADH-Glo Assay Kit (G9071; Promega). Meanwhile, the levels of cellular ATP, and NAD^+ were measured by the multiple reaction monitoring MS (MRM-MS).

Mitotracker staining and transmission electron microscopy analysis

Cells were placed in 35 mm glass bottom dish with 10 mm micro-well (Cellvis, Mountain View, CA, USA) and treated with or without GS for 48 h. After staining with Mitotracker (Beyotime Biotechnology, Shanghai, China) at 200 nM diluted in pre-warmed culture media for 30 min, cells were stained with Hoechst 33342 (Sigma-Aldrich) to mark the nuclei as previously described (Lin et al., 2015). Twenty visual fields in each well from three dishes at 400× magnification were observed by the Nikon C2 confocal microscope with ZEN software (Nikon, Tokyo, Japan), and mitochondria quantity was analzyed. For transmission electron microscopy (TEM) analysis, cells treated with or without GS were fixed in 2.5% glutaraldehyde for 1 h and then incubated with 1% osmium tetroxide. After dehydration and embedding in Durcupan Water-Soluble Embedding Medium, the specimens were sectioned into 60 nm by a diamond knife and mounted on copper grids. Micrographs were viewed by TEM (FEI Tecnai G2 20; TWIN, Hillsboro, OR, USA) to analyze and quantify the mitochondrial size and amount in each cell from four chambers by ImageJ software (NIH, Bethesda, MD, USA) (Liu et al., 2018).

Cell viability, scratch assay and reactive oxygen species measurement

After the treatment with different concentrations of GS for 48 h, cells were incubated with Cell Counting Kit 8 (CCK8) solution (10 μl/well, Glpbio, Montclair, CA, USA) at 37°C for 40 min. The absorbance at 450 nm for different wells was detected on a microplate reader (Infinite M200pro, TECAN, Zurich, Switzerland) to analyze cell viability, according to our previous study (Li et al., 2018). For the scratch assay, a straight scratch was made using a P200 pipet tip in cells treated with GS for 48 h. After washing with phosphate-buffered saline, the images of scratch area at 0 and 24 or 72 h were captured using the Olympus Viva View FL microscope (Tokyo, Japan) and analyzed to calculate the rate of scratch closure for four fields per dish from three independent experiments using ImageJ software (Graham et al., 2018). Intracellular and mitochondrial reactive oxygen species (ROS) generation of cells treated with various concentrations of GS for 48 h were detected by carboxy-H2DCFDA fluorescent probes (Beyotime Biotechnology) or MitoSOX mitochondrial superoxide indicator (Thermo Fisher Scientific) using the FACS-Calibur flow cytometer (BD Biosciences, San Jose, CA, USA).

Establishmentof hypoxia- and OGD-induced cell models

As previously reported, H9c2 cells were kept in 800 μM cobalt chloride ($CoCl_2$) medium or in serum and glucose-free 800 μM $CoCl_2$ medium for 9 h to establish hypoxia- or OGD-induced cell injury models (Huang et al., 2020).

Drosophila melanogaster activity and climbing distance assays

Wild-type Drosophila melanogaster was maintained on standard medium (50 g/L yeast, 50 g/L glucose, 0.8% agar, and 1% soy flour) at 25-26°C in 50% relative humidity under a 12:12 h light-dark cycle. The 7-day-old flies were loaded into plastic tubes containing standard food or with GS (1 mg/mL) for 7 days. Then, the sleep-waking activity of 32 flies was consecutively monitored for 24 h using the Drosophila Activity Monitoring System (Trikinetics, Waltham, MA, USA) and recorded as beam-breaks in 1-min bins for generating the number of activities. For the climbing ability assay, 30 flies in the vertical vials (110×10 mm) were acclimatized for 15 min and simultaneously tapped to the bottom of the vial for 5 sec. The climbing distance of each fly from control or GS pretreatment was recorded to obtain the average of the distance (Algarve, Assmann, Aigaki & da Cruz, 2020).

Immunohistochemical staining

For immunohistochemical (IHC) staining, the heart and brain tissues from different groups were fixed in 4% paraformaldehyde, paraffin-embedded, and sectioned into 5 μm slides, which were analyzed for SIRT1 (1:100) expression as previously described (Huang et al., 2018).

Quantitative PCR analysis

Quantitative PCR (qPCR) was performed as previously described (Jin et al., 2020). Briefly, total RNA was extracted using TRizol (Life Technologies, Frederick, MD, USA), followed by ethanol extraction. qPCR was conducted in triplicate using SYBR Green PCR reagent (Bio-Rad, Hercules, CA, USA) on the CFX96 Real-Time PCR system (Bio-Rad). PCR conditions included a denaturation step of 95°C for 5 min, followed by 40 cycles consisting for 95°C for 15 sec, 60°C for 30 sec, and 72°C for 30 sec. The primer sequences are described in Supplementary Table 2. The relative expression of each target gene was calculated by the $2^{-\Delta\Delta^{\tau}}$ method after normalization to β-Actin.

Western blot analysis

Cells or fly brain tissues were lysed in RIPA buffer (Beyotime Biotechnology) for 1 h on ice and centrifuged at 14,000 rpm to obtain the supernatants, which were measured to detect protein concentration quantified with a BCA protein assay kit (Beyotime Biotechnology). Total protein (30μg) was resolved on 10% or 12% sodium dodecyl sulfate polyacrylamide gel electrophoresis to separate different sizes of proteins, followed by eletrotransfer onto nitrocellulose membranes. The membranes were blocked in 5% non-fat milk and probed with primary antibodies overnight at 4°C. Proteins were detected using a chemiluminescent imaging system (FluorChem, ProteinSimple, San Jose, CA, USA), after incubating with the appropriate secondary antibodies for 1 h at room temperature (Huang et al., 2018).

Statistical analysis

Data are presented as the mean ± standard deviation or mean ± stanard error of the mean from at least three independent experiments. The unpaired Student's t - test for comparing two groups or one-way analysis of variance for comparing multiple groups was used to analyze statistical significance using GraphPad Prism 8 (GraphPad Software, San Diego, CA, USA). Hierarchical cluster analysis of different metabolites was performed by Python. The raw metabolomic intensity of each metabolite from two groups was transformed into the Log^2 value of normalized intensity. For all statistical analyses, a significant difference was accepted at $P< 0.05$.

Results

GS enhances MRC and ATP production in cardiomyocytes and neurons

To explore the molecular mechanism of GS on extensive cell protection, we first investigated the effects of GS on mitochondrial function by examining OCR, as a direct measure of mitochondrial respiration (Diepart, Verrax, Calderon, Feron, Jordan & Gallez, 2010). Oxygen consumption probes were used to assess the effect of GS on the rate of basal oxygen consumption in a variety of cell lines, including H9c2, primary neonatal cardiomyocytes, differentiated PC12, primary cortical neurons, L6, C2C12, HUVECs, BMSCs, osteoblast, 16HBE, and THP-1 cells. As expected, GS pretreatment for 48 h increased basal oxygen consumption by 2.0-fold in H9c2 cells, 2.8-fold in PC12 cells, 1.5-fold in neurons **(Fig. 1A and Supplementary Fig. 3A)** , 1.6-fold in C2C12 cells, and 1.5-fold in L6 cells**(Supplementary Fig. 3B)** . Meanwhile, we found that GS had no effect on basal OCR in HUVECs, BMSCs, osteoblast, 16HBE, and THP-1 cells **(Fig. 1B,Supplementary Fig. 3B-3F)** . To further assess the potential function of GS in mitochondrial oxidative capacity, we conducted a mitochondrial stress test in H9c2, PC12, and HUVECs. The pretreatment of GS at 5 μg/mL for 48 h led to increases in basal OCR, MRC, and SRC in H9c2 and PC12 cells**(Fig. 1C and Fig. 1D)** . The similar results for mitochondrial oxidative capacity were detected by Luxcel oxygen consumption probes in H9c2 and PC12 cells **(Supplementary Fig. 4A-4B)** . In HUVECs, GS pretreatment had no effects on basal OCR, MRC, and SRC**(Supplementary Fig. 4C)** . Furthermore, intracellular ATP content was examined in H9c2, PC12, and primary neurons after GS pretreatment. As shown in **Figure 1E** , GS pretreatment significantly increased ATP production in cardiomyocytes and neurons in the same manner as OCR. LC-MS analysis showed that GS at 5 μg/mL promoted relative ATP intensity and the ratio of ATP/ADP in H9c2 cells **(Fig. 1F)** . In HUVECs, GS slightly increased ATP content and had no effect on ATP/ADP ratio**(Supplementary Fig. 4D)** . To further identify the time-dependent effect of GS on energy production, the levels of basal OCR and ATP in H9c2 cells at different time points were measured after GS pretreatment for 48 h. The results in Figure 1G and 1H demonstrated that GS pretreatment for 6 h enhanced basal OCR and ATP content at concentrations of 5 and 10 μg/mL GS. In particular, basal OCR was gradually increased by GS pretreatment in time- and dose-dependent manners. Collectively, GS pretreatment enhanced MRC and ATP production in aerobic respiration- dominated cardiomyocytes and neurons, and had no obvious effect on anaerobic respiration- dominated other cell lines such as HUVECs and BMSCs.

GS significantly promote aerobic glucose metabolism in cardiomyocytes

Increased OCR and ATP production are the manifestations of enhanced energy metabolism; thus, we performed targeted metabolomic analysis of glucose metabolites by LC-MS/MS in H9c2 and HUVECs untreated or treated with GS for 48 h. A total of 15 different intermediates of glycolysis and TCA cycle, such as pyruvate, lactate, citrate, and succinate were identified in these two cell lines. In H9c2 cells, GS led to decreases of seven metabolites and increases of eight metabolites, compared with the control group **(Fig. 2A)** . The analysis of relative intensity for each metabolite showed that GS decreased the levels of fructose 6-phosphate, fructose 1, 6-bisphosphate, 3-phosphoglycerate, dihydroxyacetone phosphate, and phosphoenolpyruvate, and increased the levels of glucose 6-phosphate and pyruvate in H9c2 cells, suggesting that GS increased the conversion of glucose to pyruvate. Moreover, key metabolites of TCA cycle such as citrate, succinate, fumarate, malate, oxaloacetate, and glycolytic metabolite, lactate were clearly increased by GS pretreatment **(Fig. 2B)** , suggesting that GS mainly accelerated TCA metabolism in the cardiomyocytes. In HUVECs, only six metabolites were upregulated by GS pretreatment, including glucose-6-phosphate, fructose-6-phosphate, pyruvate, succinate, malate, and fumarate. There were no obvious differences in the other nine metabolites between the control and GS groups **(Fig. 2C, Supplementary Fig. 5A)** . These data suggest that GS mainly increased the conversion from glucose to fructose-6-phosphate and pyruvate, and enhanced the metabolic process from succinate to malate in HUVECs. Collectively, GS had more obvious effects on promoting glucose oxidation in cardiomyocytes than endothelial cells.

Multiple key enzymes regulate glucose breakdown and TCA metabolism reaction, which were examined by Western blot analysis in the control and GS-treated H9c2 cells. GS pretreatment upregulated the levels to the rate-limiting enzymes such as HK-II, PFKP, PKM2, and PDH, and did not change GAPDH expression in H9c2 cells **(Fig. 2D, Supplementary Fig. 5B)** . Mitochondrial pyruvate carriers, MPC1 and MPC2, which play a potential role in the transport of pyruvate to mitochondria, were increased by GS compared

with the control group **(Fig. 2D, Supplementary Fig. 5B)** . Furthermore, CS, the first and rate-limiting enzyme of the TCA cycle; DLST, one of the core enzymes of α-ketoglutarate dehydrogenase complex; and fumarase, a mitochondrial metabolic enzyme, were significantly higher in GS-pretreated H9c2 cells than the control group **(Fig. 2D, Supplementary Fig. 5B)** . Two isocitrate dehydrogenase isoforms in cytoplasm (IDH1) and mitochondria (IDH2) were not regulated by GS. In addition, ACO2, which is responsible for catalyzing the isomerization of citrate to isocitrate and SDHA, were decreased by GS pretreatment **(Fig. 2D, Supplementary Fig. 5B)** . Importantly, the activity of PDH, as a rate-limiting metabolic step for glucose oxidation was measured in untreated- and GS-pretreated H9c2 and HUVECS. We found a significant induction in PDH activity in GS-treated H9c2 cells and no change of PDH activity in GS-treated HUVECs compared with control cells **(Fig. 2E)** . Taken together, our findings suggest that GS pretreatment mainly accelerates glucose conversion to pyruvate, and increases pyruvate transporting to promote TCA metabolism in the cardiomyocytes. In future experiments, we will focus on the effect and molecular mechanism of GS on cardiomyocytes and neurons dominated by aerobic respiration.

GSincrease mitochondrial biogenesis incardiomyocytes and neurons

To investigate the role of GS in mitochondrial biogenesis, we first examined mitochondrial count in cardiomyocytes and neurons using the Mitotracker probe. We found that pretreatment with GS induced a significant increase in mitochondrial content in a dose-dependent manner in H9c2 cells **(Fig. 3A-3B)** and primary neurons **(Fig. 3A and 3C)** . Moreover, high-resolution micrographs of mitochondria were obtained in control and GS-pretreated H9c2 cells using TEM. As shown in**Fig. 3D-3E** , GS pretreatment at 5 μg/mL for 48 h increased the number of mitochondria in the cardiomyocytes and had no effect on the size of myocardial mitochondria, compared with control cells. To determine if the observed changes in mitochondrial respiration and biogenesis translate into altered mitochondrial function, we performed immunoblotting with antibodies against five complexes of the oxidative phosphorylation. Compared with the control group, GS induced increases in complex I-IV levels in H9c2 cells and mainly increased the levels of CII-SDHB and CI-NDUFB8 in PC12 cells **(Fig. 3F-3G)** . The enhancement of mitochondrial function can increase ROS generation, which damages the cells, so we examined ROS level in untreated- and GS-treated H9c2 cells. Flow cytometry analysis showed that GS had no significant effect on the production of intracellular and mitochondrial ROS in H9c2 cells **(Supplementary Fig. 6A)** . Additionally, mitochondrial amount and complex protein level were further investigated in HUVECs. We did not observe the effect of GS pretreatment on mitochondrial mass in HUVECs **(Supplementary Fig. 6B-6C)** . Collectively, GS preferentially promote the mitochondrial biosynthesis of cardiomyocytes and neurons, and not that of endothelial cells.

GS increase NAD^+-dependent SIRT1 activation in cardiomyocytes and neurons

NAD^+ level and its dependent deacetylase, SIRT1, play key roles in regulating mitochondrial function (Katsyuba et al., 2018). Based on the findings above, we determined if GS could alter the intracellular level of NAD^+ and regulate SIRT1 activation in cardiomyocytes and neurons. Consistent with our hypothesis, the level of NAD^+ luminescence was obviously higher in GS-treated H9c2 and primary neurons than in the control group **(Fig. 4A)** . Moreover, the targeted metabolomic analysis showed that NAD^+ level was significantly increased by GS pretreatment in H9c2 cells **(Fig. 4B)** . As reported, NAD^+-dependent SIRT1 can deacetylate and activate PGC-1α to stimulate mitochondrial biogenesis (Aquilano, Baldelli, Pagliei & Ciriolo, 2013). As shown in **Fig. 4C** , qPCR analysis showed that GS incubation for 8 h increased SIRT1 and PGC-1α mRNA levels in H9c2 and primary neurons. Western blot analysis demonstrated that GS pretreatment for 48 h led to increases in SIRT1 and its targets PGC-1α, Nrf1, and Nrf2 in H9c2 cells **(Fig. 4D)** . Furthermore, similar findings in cardiomyocytes were observed in GS-treated PC12 cells **(Fig. 4E)** . In addition, the wound-healing ability in H9c2 cells and neurons was increased by GS pretreatment, suggesting that GS promoted cell migration **(Supplementary Fig. 7A-7C)** .

Intriguingly, GS were administered to the flies and mice to further validate the function of GS in NAD^+-dependent SIRT1 activation. Consistent with the *in vitro* results, GS administration for 7 days led to a significant increase in the intensity of NAD^+ luminescence and the ratio of NAD^+/NADH in the drosophila brain compared with the control group **(Fig. 5A)** . The increased SIRT1 in response to NAD^+ was confirmed

in the brain of drosophila treated with GS **(Fig. 5B)** . Meanwhile, the number of activities and climbing distance of 30 flies fed with GS were greatly increased, compared to the control group with common food **(Fig. 5C)** . In addition, IHC staining showed that SIRT1 expression was significantly increased in the heart and brain tissues of mice after 21 days of GS administration **(Fig. 5D)** . Together, these *in vitro* and *in vivo* results indicate that GS obviously increase NAD^+-dependent SIRT1 activation in cardiomyocytes and neurons.

GS increase mitochondrial function through the SIRT1 pathway in cardiomyocytes subjected to hypoxia and OGD injuries

Generally, ischemia in the heart can cause mitochondrial dysfunction, which consequently reduces energy metabolism to cause further cardiac damage (Kalogeris, Baines, Krenz & Korthuis, 2012). To further explore the protective effect of GS against hypoxia and OGD injuries, cell viability, OCR, ATP production, mitochondrial respiration complexes, and the SIRT1-PGC-1α pathway were investigated in control, injured model, and GS-treated H9c2 cells. As shown in **Fig. 6A** , hypoxia and OGD led to decreases in H9c2 cell viability, which were slightly recovered by GS. Consistent with current results, we found that hypoxia induced by $Cocl_2$ for 9 h significantly diminished the rate of oxygen consumption and ATP production of H9c2 cells, which were lower during the process of glucose and oxygen deprivation**(Fig. 6B-6C)** . GS pretreatment for 48 h reversed the decreases of OCR and ATP level induced by hypoxia and OGD in H9c2 cells **(Fig. 6B-6C)** . Meanwhile, the levels of five mitochondrial respiratory complexes, CV-ATP5A, CIII-UQCRC2, CIV-MTCO1, CII-SDHB, and CI-NDUFB8, were decreased by hypoxia for 9 h, which were obviously recovered by GS at 10 μg/mL **(Fig. 6D-6E)** . In addition, Western blot analysis demonstrated that hypoxia and OGD led to decrease in SIRT1 and PGC-1α levels in H9c2 cells and the levels of SIRT1 and PGC-1α in GS-pretreated H9c2 cells were higher than those in the hypoxia- or OGD-induced model group **(Fig. 6F-6G)** . Taken together, these results clearly demonstrate the protective effect of GS to increase mitochondrial function against the hypoxia- or OGD-induced cardiomyocyte damage through activation of the SIRT1-PGC-1α pathway.

SIRT1 pathway is involved in GS-enhanced mitochondrial function in cardiomyocytes

To further confirm that GS regulate mitochondrial function by the activation of SIRT1, we tested whether mitochondrial respiration, ATP production, and the NAD^+-dependent SIRT1 pathway were affected by a SIRT1 inhibitor, nicotinamiede (NAM) combined with GS. Consistent with the results above, we observed increased basal or maximal mitochondrial respiration in H9c2 cells pretreated with GS for 48 h, which was significantly blocked by NAM **(Fig. 7A-7B)** . Similarly, GS-mediated increase of ATP content in H9c2 cells was inhibited by NAM**(Fig. 7C)** . For respiratory chain complexes, higher expression of three complexes, CIII-UQCRC2, CIV-MTCO1, and CII-SDHB, induced by GS was inhibited by the combination of GS with NAM **(Fig. 7D-7E)** . Importantly, GS combined with NAM significantly reduced GS-induced NAD^+ level in H9c2 cells **(Fig. 7F)** . Then, to further determine whether increased mitochondrial function by GS is mediated by the NAD^+-dependent SIRT1 pathway, we measured protein levels of SIRT1 and its targets in control, GS-, NAM-, or GS+NAM-treated H9c2 cells by Western blot analysis. As expected, GS-mediated activation of SIRT1 and its targets, PGC-1α, Nrf1, and Nrf2, were completely abrogated by the pretreatment of GS and NAM, which was similar to the control or NAM group **(Fig. 7G-7H)** . These findings suggest that the SIRT1 pathway is involved in GS-enhanced mitochondrial function in cardiomyocytes

Ginsenoside monomers increase mitochondrial function in cardiomyocytes by activating the SIRT1 pathway

As we showed, GS are a complex mixture of ginsenoside monomers of different proportions **(Supplementary Fig. 1-2)** . To further gain insight into which ginsenoside in GS promotes mitochondrial function through increased glucose oxidation and SIRT1 activation, we performed a series of experiments to investigate the effects of different ginsenosides on basal OCR, ATP content, and key protein levels in H9c2 cells. Similar to that of GS, different ginsenoside monomers, such as Rg1, Re, Rf, Rb1, Rc, Rh1, Rb2, Rb3, Rd, S-Rg3, R-Rg3, and Rk1, at individual concentrations of GS increased basal OCR in H9c2 cells after 48 h treatment

compared with the control group **(Fig. 8A)** . Moreover, ATP content was higher in Re-, Rf-, Rb1-, Rc-, Rh1-, Rb2-, or Rb3-treated H9c2 cells than the control or GS group **(Fig. 8B)** . These results confirm that these ginsenosides can promote mitochondrial energy metabolism. Additionally, key proteins of the glucose oxidation process, HK-II and MPC1, were increased by Rg1, Re, Rf, and Rc, which was similar to GS **(Fig. 8C-8D)** . For SIRT1 expression, we found that the level of SIRT1 was upregulated by most of the ginsenoside monomers, with the exception of Rk3 **(Fig. 8C-8D)** . Especially, ginsenosides Rg1, Re, Rc, Rh1, Rb2, and Rb3 had a similar role in increasing SIRT1 expression as GS **(Fig. 8C-8D)** . Taken together, these results identified the major ginsenosides in GS, including Rg1, Re, Rf, Rb1, Rc, Rh1, Rb2, and Rb3, which promote aerobic cellular respiration and SIRT1-mediated mitochondrial biosynthesis to protect cardiomyocytes.

Discussion

Here, we revealed the novel mechanism by which GS promote mitochondrial energy metabolism in cardiomyocytes and neurons, aerobic respiration- dominated cells. In this study, GS pretreatment increased mitochondrial aerobic respiration, ATP production, and cellular NAD^+level. Moreover, GS activated the SIRT1-PGC-1α pathway to promote mitochondrial biosynthesis and ETC complex II-IV levels, which was inhibited by NAM. In hypoxia- and OGD-induced cell injuries, GS also increased ATP content and OXPHOS protein levels by promoting the activation of the SIRT1-PGC-1α pathway. Finally, major ginsenoside monomers in GS were identified for increasing HK-II, MPC1, and SIRT1 levels to promote mitochondrial energy promotion. These findings confirmed the potential role of GS for energy metabolism, which supported the clinical application of ginseng for the benefit of human health and ischemic disorders **(Fig. 9)** .

As previously reported, ginsenosides have potential health benefits in improving immunity and energy, and combating cardiovascular, cerebrovascular, and metabolic diseases (Ratan et al., 2020), which might be associated with the enhancement of glucose energy metabolism. In individual cell types, glycolysis and OXPHOS are utilized to maintain energy metabolic needs. Several studies have demonstrated that neurons depend on mitochondria, and endothelial cells rely on glycolysis, whereas skeletal cells utilize both OXPHOS and glycolysis for energy supply (Chang, Singh, Gross & Kioussi, 2019; De Bock et al., 2013; Zeiger, Stankowski & McLaughlin, 2011). For the first time, we chose a couple of types of cell lines such as cardiomyocytes (H9c2, primary cardiac myocytes), neurons (differentiated PC12, primary neurons), bone marrow-derived stem cells, endotheliocytes (HUVECs), and stem cells to determine the effect of GS on energy metabolism. The analysis of basal OCR demonstrated that GS preferably increased oxygen consumption in cells, cardiomyocytes, and neurons, which were highly dependent on mitochondria, not those cell lines depdendent on glycolysis for energy production, such as endothelial cells, or stem cells. Furthermore, ATP measurement and mitochondrial stress assay confirm the preferable effect of GS on mitochondrial respiration-dominant cardiomyocytes and neurons, similar to previous findings that ginseng extract containing Rg1, Re, Rb1, and Rd can promote the OCR and ATP production in healthy cardiomyocytes (Huang et al., 2019).

Glucose 6-phosphate is an essential metabolite in the first step of glucose metabolism, which is converted from glucose by hexokinases (John, Weiss & Ribalet, 2011). During the early stage of glycolysis, the content of glucose-6-phosphate was increased by GS in both cell lines. However, other major metabolites before pyruvate were obviously decreased in cardiomyocytes and not in endothelial cells. It suggests that the rapid metabolic process from fructose 6-phosphate to pyruvate was induced by GS in cardiomyocytes, which may be related to GS-mediated high expression of key rate-limiting enzymes, HK-II, PFKP, and PKM2. Meanwhile, pyruvate transport to mitochondria medicated by MPC1/2 and its conversion into acetyl-CoA by PDH were enhanced by GS in cardiomyocytes, similar to the functions of Rb1 (Li et al., 2017) and Rg5 (Peng et al., 2019). PDH is a vital regulatory enzyme for the connection of glycolysis to the aerobic TCA cycle, which was activated by GS in cardiomyocytes, not in endothelial cells. As previously reported from heart tissue proteome and urine metabolome, total ginsenosides or ginseng extract can modulate the levels of TCA cycle proteins, such as pyruvate dehydrogenase complex in rat heart tissues (Wang, Zhou, Yi, Jiang & Liu, 2012; Yang et al., 2016), which was deeply confirmed by our study. In addition, multiple metabolites in cardiomyocytes from succinate to citrate were increased by GS, but GS only enhanced the metabolic process from succinate to malate in endothelial cells. Compared with current reports, our findings clearly explore the

role of GS on energy metabolism that GS pretreatment preferably promotes glucose metabolism into the TCA cycle for providing energy in cardiomyocytes, and has a slight function in endothelial cells through regulating different key enzymes in a series of steps of glucose metabolism. During the OXPHOS, for the first time, we found that GS mainly promoted the expressions of ETC complex proteins I-IV to increase the transfer of electrons in the inner membrane of mitochondria, which were not changed in endothelial cells. Currently, only one previous report has shown that ginsenoside Re can rescue complex IV deficiency in PINK1 null neuronal cells (Kim, Song, Yoon, Shehzad, Kim & Son, 2012). However, we need to perform the ^{13}C-based metabolic flux analysis to identify the accurate mapping of GS-mediated aerobic glucose oxidation in the future.

NAD^+ can modulate glycolysis in the cytoplasm and the TCA cycle/OXPHOS in the mitochondria, and activate sirtuins to maintain energy homeostasis (Canto, Menzies & Auwerx, 2015). In our study, NAD^+ levels in the cardiomyocytes, primary neurons, and fly brains were increased by GS treatment, which can activate SIRT1 to match cellular energy requirements (Canto & Auwerx, 2012). SIRT1-mediated deacetylation leads to higher levels of PGC-1a to induce the nuclear transcription of Nrf1/2 for mitochondrial biogenesis (Canto & Auwerx, 2012). In different models, we found that SIRT1 and its downstream pathway were obviously activated by GS, which may be the molecular mechanism of GS on the induction of mitochondrial mass. As we showed, GS-mediated mitochondrial respiration, ATP production, and higher levels of ETC proteins were abolished by NAM, which confirm that GS promote mitochondrial biosynthesis and function through the activation of SIRT1 pathway. In the stress conditions, such as hypoxia or OGD, we obtained similar findings that GS can activate the SIRT1-PGC-1α pathway to increase the levels of all five complexes and mitochondrial bioenergetics to maintain energy homeostasis in cardiomyocytes, which may be one of the potential mechanisms of GS against ischemic disorders. Many studies demonstrate that ginsenoside Rg3 or a prescription containing ginseng could enhance mitochondrial respiration in healthy and unhealthy cells (Lin et al., 2015; Sun et al., 2013). Our results together with previous findings can verify the beneficial functions of ginsenosides on mitochondrial energy metabolism without ROS injury.

For glucose oxidation, very few ginsenosides, such as compound K, Rg3, or Rg5, can regulate HK-II expression to inhibit tumor growth or protect cardiomyocyte ischemic injury (Chen et al., 2019a; Yang et al., 2017). In our study, we found that other ginsenosides Rg1, Re, Rf, and Rc can upregulate HK-II level. For SIRT1 activation, ginsenoside monomers, including Rb1, Rb2, Rc, and Rg3, have been identified as potential SIRT1 activators (Wang, Liang, Chen & Zhao, 2016; Yang, Ma, Zhou, Xu & Zhang, 2017). Ginsenoside Rb2, Rc, and F1 can promote SIRT1 activation to increase ATP production and inhibit oxidative stress in cardiomyocytes (Wang, Liang, Chen & Zhao, 2016). Another study showed that ginsenosides Rg1, Rb1, Re, Rh2, Rg3, and Rg5 can protect ischemic brain injury, which is associated with STIRT1 activation and Toll-like receptor 4/myeloid differentiation factor 88 signaling pathways (Cheng et al., 2019). In our study, we found that most ginsenosides can activate SIRT1 and enhance ATP content, similar to previous findings. According to the content percentage of each ginsenoside in GS, we found that Rh1, Rb3, Rb2, or Rf at the concentration of lower than 0.2 μg/mL had a good effect on SIRT1 activation and mitochondrial respiration. Moreover, the analysis from published findings speculated that two glucopyranosyl groups on the C-3 position of ginsenosides are critical for SIRT1 activity (Ma, Zhou & Yang, 2015; Wang, Liang, Chen & Zhao, 2016; Yang, Ma, Zhou, Xu & Zhang, 2017). Therefore, the binding mechanism of ginsenosides on the SIRT1 needs to be well studied to explore the sites of key amino acids in SIRT1 proteins using molecular docking, protein interaction, and mutation techniques. More importantly, the synergistic effects of different ginsenosides targeting potential molecules of glucose metabolism and SIRT1 pathway could be investigated in the future.

Conclusion

In summary, *in vitro* and *in vivo* data provided evidence that GS from *Panax* ginseng promoted aerobic cellular respiration and SIRT1-mediated mitochondrial biosynthesis in cardiomyocytes and neurons. Major ginsenoside monomers, such as Rb1, Rb2, Rb3, Rc, Rd, Re, Rf, or Rg1, in GS were found to activate mitochondrial respiration and SIRT1 pathway to promote energy metabolism. This study provides new

insights into the extensive application of ginseng for cardiac and neurological protection in healthy subjects and patients with ischemic disorders.

Source of funding

This study was supported by the National Key Research and Development Program of China (2017YFC1702103), National Natural Science Foundation of China (U19A2013) and the Science and Technology Development Plan Project of Jilin Province (202002053JC, 20190101010JH, and 20180623041TC), the Project for Science and Technology Bureau of Changchun (18YJ013) and Jilin Provincial Administration of Traditional Chinese Medicine (2020168).

Author contributions

DZ and XL: conceived and designed this study. LS, DZ, and XL: participated in the study design and interpreted data. QH and XL: prepared the draft manuscript. QH, TL, JL, MW, XC, LX, XT, WQ, ZZ, HS, WJ, and CJ: participated in the data collection and analysis. DZ and XL: funding support. All authors have read and approved final manuscript.

Declaration of transparency and scientific rigour

This Declaration acknowledges that this paper adheres to the principles for transparent reporting and scientific rigour of preclinical research as stated in the *BJP* guidelines for Natural Products Research, Design and Analysis, Immunoblotting and Immunochemistry, and Animal Experimentation, and as recommended by funding agencies, publishers and other organisations engaged with supporting research.

Data availability statement

The data that support the findings of this study are available from the corresponding author upon reasonable request.

References

Algarve TD, Assmann CE, Aigaki T, & da Cruz IBM (2020). Parental and preimaginal exposure to methylmercury disrupts locomotor activity and circadian rhythm of adult Drosophila melanogaster. Drug Chem Toxicol 43**:** 255-265.

Almeida A, Delgado-Esteban M, Bolanos JP, & Medina JM (2002). Oxygen and glucose deprivation induces mitochondrial dysfunction and oxidative stress in neurones but not in astrocytes in primary culture. J Neurochem 81**:** 207-217.

Aquilano K, Baldelli S, Pagliei B, & Ciriolo MR (2013). Extranuclear localization of SIRT1 and PGC-1alpha: an insight into possible roles in diseases associated with mitochondrial dysfunction. Curr Mol Med 13**:** 140-154.

Aravinthan A, Kim JH, Antonisamy P, Kang CW, Choi J, Kim NS*, et al.* (2015). Ginseng total saponin attenuates myocardial injury via anti-oxidative and anti-inflammatory properties. J Ginseng Res 39**:** 206-212.

Baccelli I, Gareau Y, Lehnertz B, Gingras S, Spinella JF, Corneau S*, et al.* (2019). Mubritinib Targets the Electron Transport Chain Complex I and Reveals the Landscape of OXPHOS Dependency in Acute Myeloid Leukemia. Cancer Cell 36**:**84-99 e88.

Bricker DK, Taylor EB, Schell JC, Orsak T, Boutron A, Chen YC*, et al.* (2012). A mitochondrial pyruvate carrier required for pyruvate uptake in yeast, Drosophila, and humans. Science 337**:** 96-100.

Butterfield DA, & Halliwell B (2019). Oxidative stress, dysfunctional glucose metabolism and Alzheimer disease. Nat Rev Neurosci 20**:** 148-160.

Canto C, & Auwerx J (2012). Targeting sirtuin 1 to improve metabolism: all you need is NAD(+)? Pharmacol Rev 64**:** 166-187.

Canto C, Menzies KJ, & Auwerx J (2015). NAD(+) Metabolism and the Control of Energy Homeostasis: A Balancing Act between Mitochondria and the Nucleus. Cell Metab 22**:** 31-53.

Chang CN, Singh AJ, Gross MK, & Kioussi C (2019). Requirement of Pitx2 for skeletal muscle homeostasis. Dev Biol 445**:** 90-102.

Chen HF, Wu LX, Li XF, Zhu YC, Wang WX, Xu CW*, et al.* (2019a). Ginsenoside compound K inhibits growth of lung cancer cells via HIF-1alpha-mediated glucose metabolism. Cell Mol Biol (Noisy-le-grand) 65**:** 48-52.

Chen X, Wang Q, Shao M, Ma L, Guo D, Wu Y*, et al.* (2019b). Ginsenoside Rb3 regulates energy metabolism and apoptosis in cardiomyocytes via activating PPARalpha pathway. Biomed Pharmacother 120**:** 109487.

Cheng Z, Zhang M, Ling C, Zhu Y, Ren H, Hong C*, et al.* (2019). Neuroprotective Effects of Ginsenosides against Cerebral Ischemia. Molecules 24.

De Bock K, Georgiadou M, Schoors S, Kuchnio A, Wong BW, Cantelmo AR*, et al.* (2013). Role of PFKFB3-driven glycolysis in vessel sprouting. Cell 154**:**651-663.

Di Lisa F, Canton M, Menabo R, Kaludercic N, & Bernardi P (2007). Mitochondria and cardioprotection. Heart Fail Rev 12**:** 249-260.

Diepart C, Verrax J, Calderon PB, Feron O, Jordan BF, & Gallez B (2010). Comparison of methods for measuring oxygen consumption in tumor cells in vitro. Anal Biochem 396**:** 250-256.

Dong G, Chen T, Ren X, Zhang Z, Huang W, Liu L*, et al.* (2016). Rg1 prevents myocardial hypoxia/reoxygenation injury by regulating mitochondrial dynamics imbalance via modulation of glutamate dehydrogenase and mitofusin 2. Mitochondrion 26**:** 7-18.

Fernie AR, Carrari F, & Sweetlove LJ (2004). Respiratory metabolism: glycolysis, the TCA cycle and mitochondrial electron transport. Curr Opin Plant Biol 7**:**254-261.

Fillmore N, & Lopaschuk GD (2013). Targeting mitochondrial oxidative metabolism as an approach to treat heart failure. Biochim Biophys Acta 1833**:** 857-865.

Graham DM, Andersen T, Sharek L, Uzer G, Rothenberg K, Hoffman BD*, et al.* (2018). Enucleated cells reveal differential roles of the nucleus in cell migration, polarity, and mechanotransduction. The Journal of cell biology 217**:**895-914.

Hall CN, Klein-Flugge MC, Howarth C, & Attwell D (2012). Oxidative phosphorylation, not glycolysis, powers presynaptic and postsynaptic mechanisms underlying brain information processing. J Neurosci 32**:** 8940-8951.

Hickey AJ, Chai CC, Choong SY, de Freitas Costa S, Skea GL, Phillips AR*, et al.* (2009). Impaired ATP turnover and ADP supply depress cardiac mitochondrial respiration and elevate superoxide in nonfailing spontaneously hypertensive rat hearts. Am J Physiol Cell Physiol 297**:** C766-774.

Hopp AK, Gruter P, & Hottiger MO (2019). Regulation of Glucose Metabolism by NAD(+) and ADP-Ribosylation. Cells 8.

Huang Q, Lan T, Lu J, Zhang H, Zhang D, Lou T*, et al.* (2018). DiDang Tang Inhibits Endoplasmic Reticulum Stress-Mediated Apoptosis Induced by Oxygen Glucose Deprivation and Intracerebral Hemorrhage Through Blockade of the GRP78-IRE1/PERK Pathways. Front Pharmacol 9**:** 1423.

Huang Q, Lou T, Wang M, Xue L, Lu J, Zhang H*, et al.* (2020). Compound K inhibits autophagy-mediated apoptosis induced by oxygen and glucose deprivation/reperfusion via regulating AMPK-mTOR pathway in neurons. Life Sci 254**:** 117793.

Huang Y, Kwan KKL, Leung KW, Yao P, Wang H, Dong TT*, et al.* (2019). Ginseng extracts modulate mitochondrial bioenergetics of live cardiomyoblasts: a functional comparison of different extraction solvents. J Ginseng Res 43**:**517-526.

Imai S, & Guarente L (2014). NAD+ and sirtuins in aging and disease. Trends Cell Biol 24**:**464-471.

Irrcher I, Adhihetty PJ, Sheehan T, Joseph AM, & Hood DA (2003). PPARgamma coactivator-1alpha expression during thyroid hormone- and contractile activity-induced mitochondrial adaptations. Am J Physiol Cell Physiol 284**:** C1669-1677.

Jia Y, Zhang S, Huang F, & Leung SW (2012). Could ginseng-based medicines be better than nitrates in treating ischemic heart disease? A systematic review and meta-analysis of randomized controlled trials. Complement Ther Med 20**:**155-166.

Jin W, Zhu X, Yao F, Xu X, Chen X, Luo Z*, et al.* (2020). Cytoprotective effect of Fufang Lurong Jiangu capsule against hydrogen peroxide-induced oxidative stress in bone marrow stromal cell-derived osteoblasts through the Nrf2/HO-1 signaling pathway. Biomed Pharmacother 121**:** 109676.

John S, Weiss JN, & Ribalet B (2011). Subcellular localization of hexokinases I and II directs the metabolic fate of glucose. PLoS One 6**:** e17674.

Kalogeris T, Baines CP, Krenz M, & Korthuis RJ (2012). Cell biology of ischemia/reperfusion injury. Int Rev Cell Mol Biol 298**:** 229-317.

Katsyuba E, Mottis A, Zietak M, De Franco F, van der Velpen V, Gariani K*, et al.* (2018). De novo NAD(+) synthesis enhances mitochondrial function and improves health. Nature 563**:** 354-359.

Kim KH, Song K, Yoon SH, Shehzad O, Kim YS, & Son JH (2012). Rescue of PINK1 protein null-specific mitochondrial complex IV deficits by ginsenoside Re activation of nitric oxide signaling. J Biol Chem 287**:** 44109-44120.

Li J, Yang YL, Li LZ, Zhang L, Liu Q, Liu K*, et al.* (2017). Succinate accumulation impairs cardiac pyruvate dehydrogenase activity through GRP91-dependent and independent signaling pathways: Therapeutic effects of ginsenoside Rb1. Biochim Biophys Acta Mol Basis Dis 1863**:** 2835-2847.

Li X, Huang Q, Wang M, Yan X, Song X, Ma R*, et al.* (2018). Compound K Inhibits Autophagy-Mediated Apoptosis Through Activation of the PI3K-Akt Signaling Pathway Thus Protecting Against Ischemia/Reperfusion Injury. Cell Physiol Biochem 47**:** 2589-2601.

Lin S, Wu X, Tao L, Bei Y, Zhang H, Zhou Y*, et al.* (2015). The Metabolic Effects of Traditional Chinese Medication Qiliqiangxin on H9C2 Cardiomyocytes. Cell Physiol Biochem 37**:** 2246-2256.

Liu D, Ma Z, Di S, Yang Y, Yang J, Xu L*, et al.* (2018). AMPK/PGC1alpha activation by melatonin attenuates acute doxorubicin cardiotoxicity via alleviating mitochondrial oxidative damage and apoptosis. Free Radic Biol Med 129**:** 59-72.

Liu L, Anderson GA, Fernandez TG, & Dore S (2019). Efficacy and Mechanism of Panax Ginseng in Experimental Stroke. Front Neurosci 13**:** 294.

Louch WE, Sheehan KA, & Wolska BM (2011). Methods in cardiomyocyte isolation, culture, and gene transfer. J Mol Cell Cardiol 51**:** 288-298.

Ma LY, Zhou QL, & Yang XW (2015). New SIRT1 activator from alkaline hydrolysate of total saponins in the stems-leaves of Panax ginseng. Bioorg Med Chem Lett 25**:**5321-5325.

Ma S, Feng J, Zhang R, Chen J, Han D, Li X*, et al.* (2017). SIRT1 Activation by Resveratrol Alleviates Cardiac Dysfunction via Mitochondrial Regulation in Diabetic Cardiomyopathy Mice. Oxid Med Cell Longev 2017**:** 4602715.

Mitsuishi Y, Taguchi K, Kawatani Y, Shibata T, Nukiwa T, Aburatani H*, et al.* (2012). Nrf2 redirects glucose and glutamine into anabolic pathways in metabolic reprogramming. Cancer Cell 22**:** 66-79.

Narne P, Pandey V, & Phanithi PB (2017). Interplay between mitochondrial metabolism and oxidative stress in ischemic stroke: An epigenetic connection. Mol Cell Neurosci 82**:** 176-194.

Neubauer S (2007). The failing heart–an engine out of fuel. N Engl J Med 356**:** 1140-1151.

Papandreou I, Cairns RA, Fontana L, Lim AL, & Denko NC (2006). HIF-1 mediates adaptation to hypoxia by actively downregulating mitochondrial oxygen consumption. Cell Metab 3**:** 187-197.

Peng S, Wang Y, Zhou Y, Ma T, Wang Y, Li J*, et al.* (2019). Rare ginsenosides ameliorate lipid overload-induced myocardial insulin resistance via modulating metabolic flexibility. Phytomedicine 58**:** 152745.

Ratan ZA, Haidere MF, Hong YH, Park SH, Lee J-O, Lee J*, et al.* (2020). Pharmacological potential of ginseng and its major component ginsenosides. Journal of Ginseng Research.

Song Z, Liu Y, Hao B, Yu S, Zhang H, Liu D*, et al.* (2014). Ginsenoside Rb1 prevents H2O2-induced HUVEC senescence by stimulating sirtuin-1 pathway. PLoS One 9**:**e112699.

Sugden MC, & Holness MJ (2003). Recent advances in mechanisms regulating glucose oxidation at the level of the pyruvate dehydrogenase complex by PDKs. Am J Physiol Endocrinol Metab 284**:** E855-862.

Sun M, Huang C, Wang C, Zheng J, Zhang P, Xu Y*, et al.* (2013). Ginsenoside Rg3 improves cardiac mitochondrial population quality: mimetic exercise training. Biochem Biophys Res Commun 441**:** 169-174.

Tang Y, Luo B, Deng Z, Wang B, Liu F, Li J*, et al.* (2016). Mitochondrial aerobic respiration is activated during hair follicle stem cell differentiation, and its dysfunction retards hair regeneration. PeerJ 4**:** e1821.

Wallace DC, Fan W, & Procaccio V (2010). Mitochondrial energetics and therapeutics. Annu Rev Pathol 5**:** 297-348.

Wang JR, Zhou H, Yi XQ, Jiang ZH, & Liu L (2012). Total ginsenosides of Radix Ginseng modulates tricarboxylic acid cycle protein expression to enhance cardiac energy metabolism in ischemic rat heart tissues. Molecules 17**:**12746-12757.

Wang QL, Yang L, Peng Y, Gao M, Yang MS, Xing W*, et al.* (2019). Ginsenoside Rg1 Regulates SIRT1 to Ameliorate Sepsis-Induced Lung Inflammation and Injury via Inhibiting Endoplasmic Reticulum Stress and Inflammation. Mediators Inflamm 2019**:** 6453296.

Wang Y, Liang X, Chen Y, & Zhao X (2016). Screening SIRT1 Activators from Medicinal Plants as Bioactive Compounds against Oxidative Damage in Mitochondrial Function. Oxid Med Cell Longev 2016**:** 4206392.

Wheaton WW, & Chandel NS (2011). Hypoxia. 2. Hypoxia regulates cellular metabolism. Am J Physiol Cell Physiol 300**:** C385-393.

Wu T, Kwaku OR, Li H-Z, Yang C-R, Ge L-J, & Xu M (2019). Sense Ginsenosides From Ginsengs: Structure-Activity Relationship in Autophagy. Natural Product Communications 14.

Wu Z, Puigserver P, Andersson U, Zhang C, Adelmant G, Mootha V*, et al.* (1999). Mechanisms controlling mitochondrial biogenesis and respiration through the thermogenic coactivator PGC-1. Cell 98**:** 115-124.

Xu M, Ma Q, Fan C, Chen X, Zhang H, & Tang M (2019). Ginsenosides Rb1 and Rg1 Protect Primary Cultured Astrocytes against Oxygen-Glucose Deprivation/Reoxygenation-Induced Injury via Improving Mitochondrial Function. Int J Mol Sci 20.

Yang JL, Mukda S, & Chen SD (2018). Diverse roles of mitochondria in ischemic stroke. Redox Biol 16**:** 263-275.

Yang L, Yu QT, Ge YZ, Zhang WS, Fan Y, Ma CW*, et al.* (2016). Distinct urine metabolome after Asian ginseng and American ginseng intervention based on GC-MS metabolomics approach. Sci Rep 6**:** 39045.

Yang XW, Ma LY, Zhou QL, Xu W, & Zhang YB (2017). SIRT1 activator isolated from artificial gastric juice incubate of total saponins in stems and leaves of Panax ginseng. Bioorg Med Chem Lett.

Yang YL, Li J, Liu K, Zhang L, Liu Q, Liu B*, et al.* (2017). Ginsenoside Rg5 increases cardiomyocyte resistance to ischemic injury through regulation of mitochondrial hexokinase-II and dynamin-related protein 1. Cell Death Dis 8**:**e2625.

Yepez VA, Kremer LS, Iuso A, Gusic M, Kopajtich R, Konarikova E*, et al.* (2018). OCR-Stats: Robust estimation and statistical testing of mitochondrial respiration activities using Seahorse XF Analyzer. PLoS One 13**:** e0199938.

Zeiger SL, Stankowski JN, & McLaughlin B (2011). Assessing neuronal bioenergetic status. Methods Mol Biol 758**:** 215-235.

Zhao XY, Lu MH, Yuan DJ, Xu DE, Yao PP, Ji WL*, et al.* (2019). Mitochondrial Dysfunction in Neural Injury. Front Neurosci 13**:** 30.

Zhou Y, Wang S, Li Y, Yu S, & Zhao Y (2017). SIRT1/PGC-1alpha Signaling Promotes Mitochondrial Functional Recovery and Reduces Apoptosis after Intracerebral Hemorrhage in Rats. Front Mol Neurosci 10**:** 443.

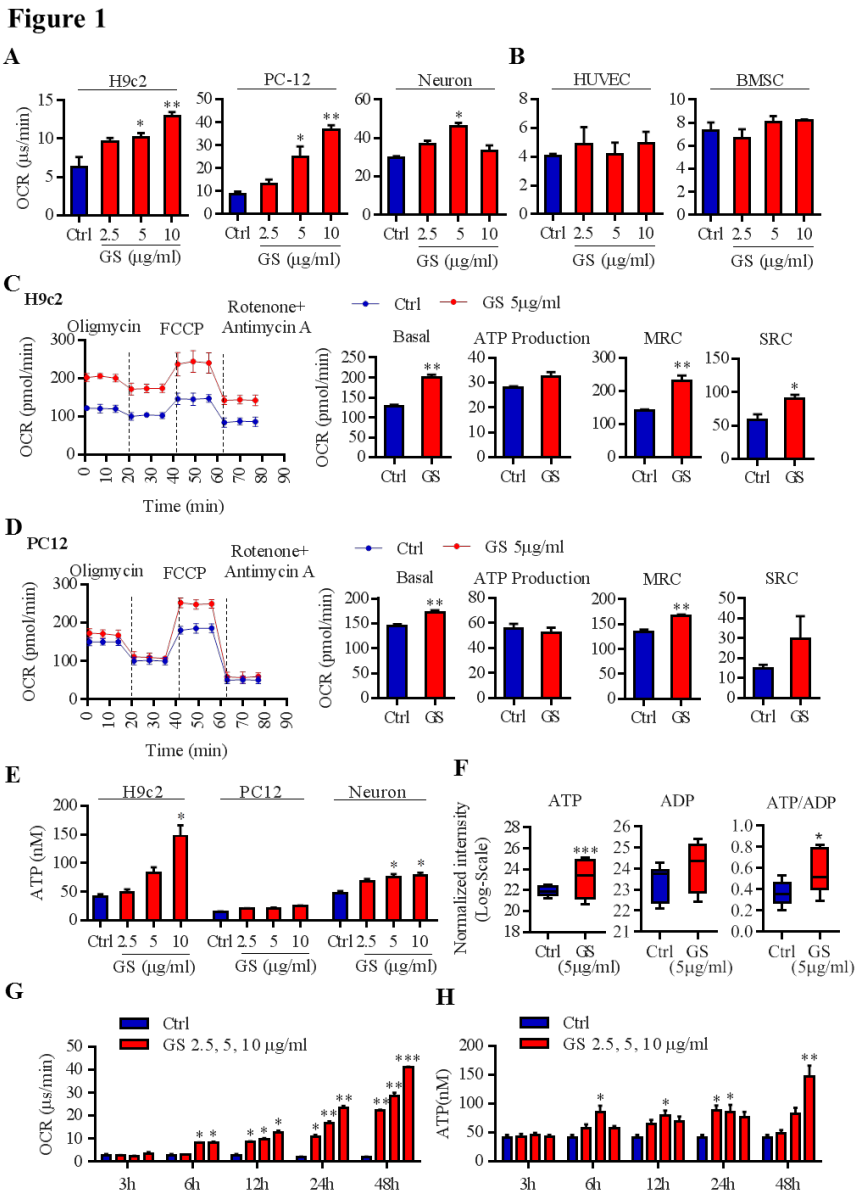

Fig. 1. GS enhanced mitochondrial respiration capacity and ATP production in cardiomyocytes and neurons. (A-B) Basal oxygen consumption rate (OCR) in H9c2, NGF-induced PC12, neuron, HUVECs and BMSCs treated with different concentrations of total ginsenosides (GS) for 48 h was measured using a MitoXpress® Xtra probe normalized to cell number. **(C)**OCR was analyzed at basal condition and sequential injections of oligomycin (1 μM), FCCP (5 μM), rotenone (Rot, 1 μM) and antimycin A (AA, 1 μM) in control and GS-pretreated H9c2 cells by the MitoStress Test Kit. After the normalization to cell number, basal OCR, ATP production, maximal respiratory capacity (MRC), and spare respiratory capacity (SRC) were calculated and shown. **(D)** Similar to the panel C, basal OCR, ATP production, MRC, and SRC were analyzed in NGF-induced PC12 cells, after GS pretreatment for 48 h. **(E)** After pretreatment with GS at 2.5, 5, or 10 μg/mL for 48 h, ATP levels in H9c2, PC12, and neurons were measured by the Bioluminescence Detection Kit. **(F)**The intensities of ATP and ADP in control and GS-treated H9c2 cells were analyzed by

the LC-MS/MS method based on MRM detection. The ratio of ATP and ADP was calculated and shown. **(G-H)** Basal OCR and ATP content in H9c2 cells treated with different concentrations (2.5, 5, or 10 μg/mL) of GS and incubated for 3, 6, 12, 24, or 48 h were measured as described as the methods above. Ctrl: control group. $^{*}P < 0.05$, $^{**}P < 0.01$, and $^{***}P < 0.001$ *versus* Ctrl group.

Figure 2

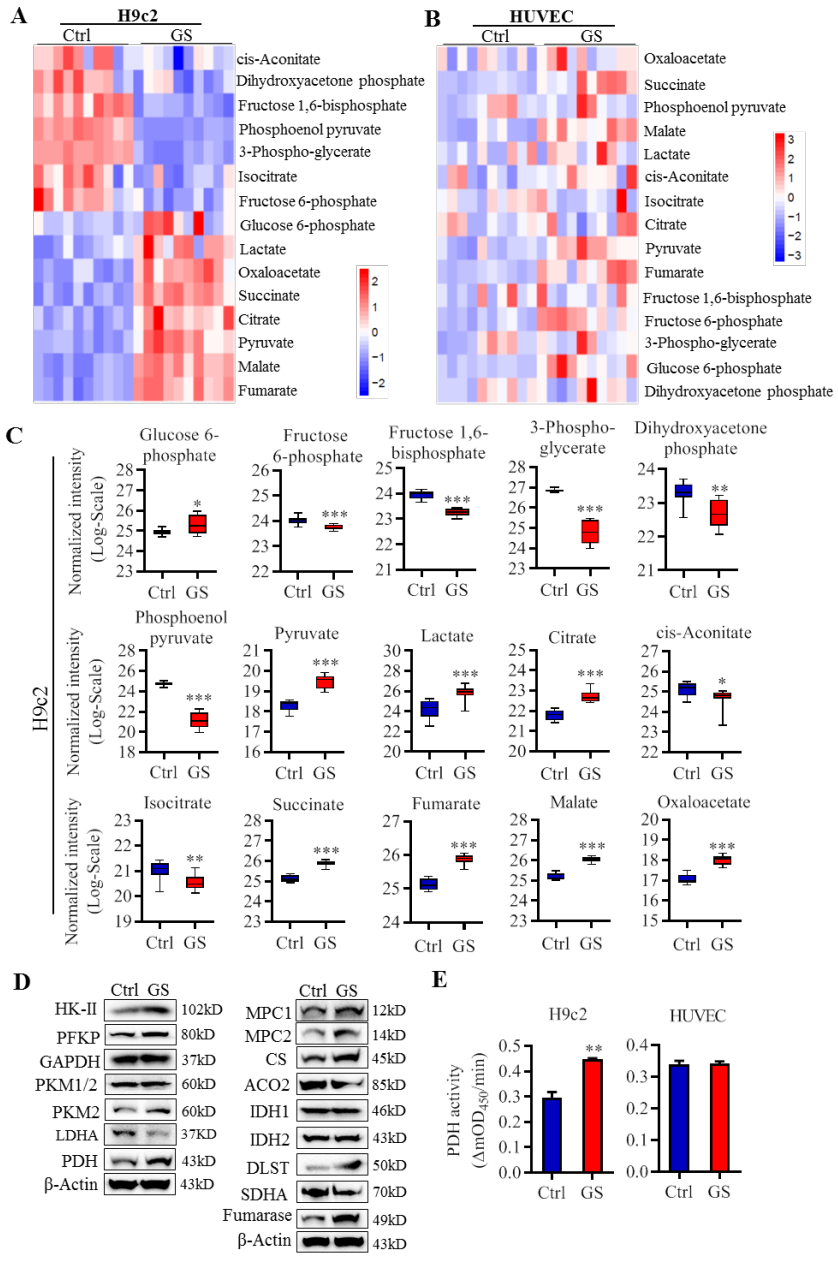

Fig. 2. Effect of GS on key metabolites and enzymes of glucose metabolism in H9c2 and HUVECs.(A) The heatmap represents the targeted metabolomic analysis of 15 key metabolites of glucose metabolism in control and GS-pretreated H9c2 cells, after 48 h incubation.**(B)** Bar graph depicts the quantification of 15 metabolites in H9c2 cells in control and GS-pretreated H9c2 cells. **(C)** The heatmap showing

15 metabolites of glucose metabolism in control and GS-pretreated HUVECs.**(D)** After GS pretreatment for 48 h, key enzymes of glycolysis and TCA cycle and mitochondrial pyruvate carriers were detected by Western blot analysis. **(E)** Pyruvate dehydrogenase (PDH) activities in H9c2 and HUVECs cells pretreated with GS for 48 h were measured. Ctrl: control group. $^{*}P < 0.05$, $^{**}P < 0.01$, and $^{***}P < 0.001$ *versus* Ctrl group.

Figure 3

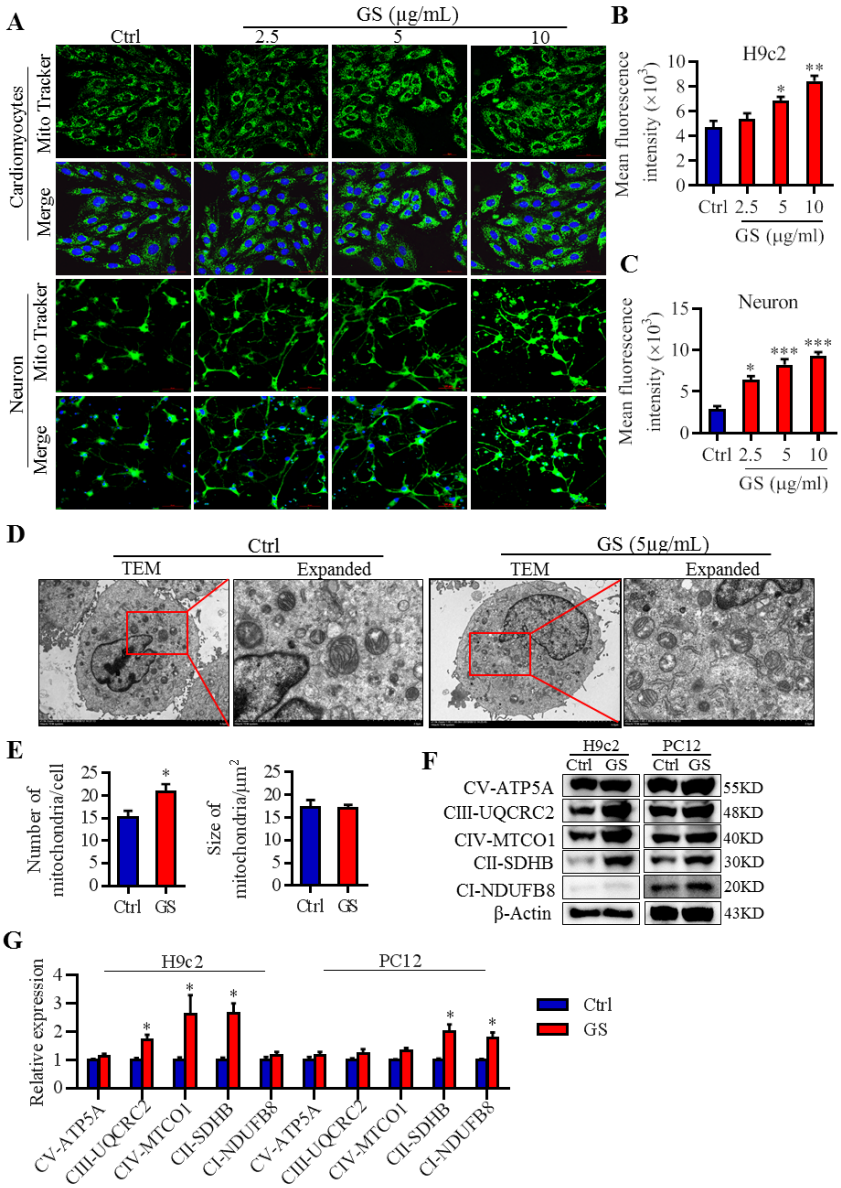

Fig. 3. GS increase mitochondrial biogenesis in cardiomyocytes and neurons. **(A)** After GS pretreatment for 48 h, H9c2 and neurons were co-stained with MitoTracker Green probe and Hoechst 33342 to analyze mitochondria amount by confocal microscopy.**(B-C)** Quantitative analysis of mitochondrial fluorescence intensity in control and GS-pretreated H9c2 and neurons from (A).**(D-E)** Mitochondrial structure in control and GS-treated H9c2 cells was observed by a transmission electron microscope. The number and

size of mitochondria in H9c2 cells from different groups were analyzed by ImageJ. **(F)** After incubation with GS at 5 μg/mL for 48 h, the levels of mitochondrial complexes I-V in H9c2 and PC12 cells were detected by Western blot analysis. **(G)** Relative expressions of complexes I-V in H9c2 and PC12 cells from (F) were quantified. Ctrl: control group. $^{*}P < 0.05$, $^{**}P < 0.01$, $^{***}P < 0.001$ *versus* Ctrl group. CI-NDUFB8: NADH dehydrogenase 1 beta subcomplex subunit 8, CII-SDHB: succinate dehydrogenase iron-sulfur subunit, CIII-UQCRC2: ubiquinol-cytochrome-c reductase complex core protein 2, CIV-MTCO1: mitochondrially encoded cytochrome C oxidase I, CV-ATP5A: ATP synthase F1 subunit α.

Figure 4

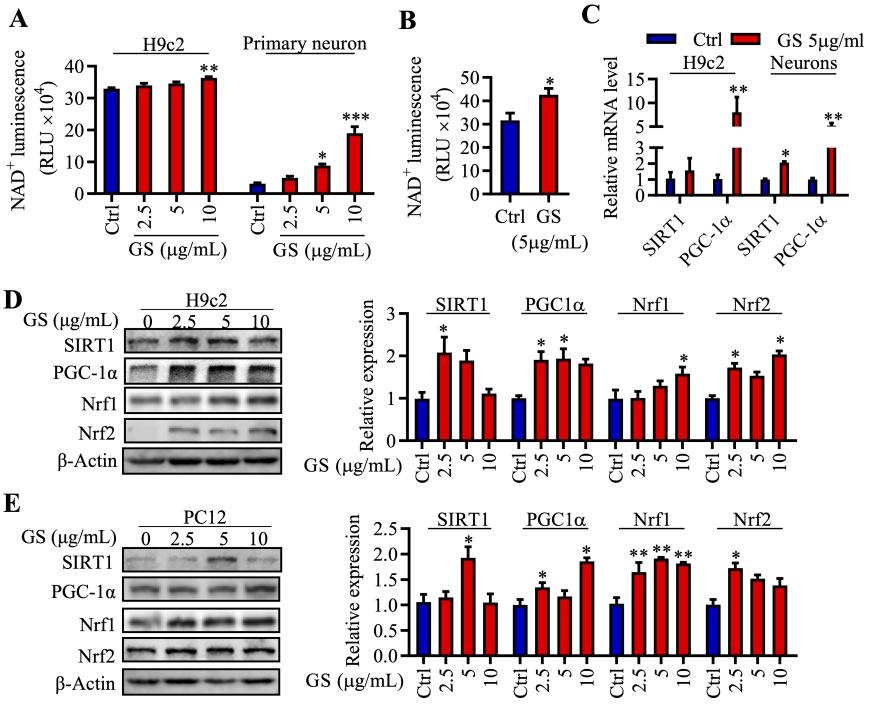

Fig. 4. GS promote NAD^{+}-dependent SIRT1 activation in cardiomyocytes and neurons . **(A)** The NAD^{+} levels in H9c2 and neurons treated with different concentrations of GS for 48 h were measured by a luminescence -based kit. **(B)** The NAD level in control and GS-treated H9c2 cells was analyzed by the LC-MS/MS method. **(C)** After GS treatment for 8 h, SIRT1 and PGC-1α mRNA levels in H9c2 cells and primary neurons were analyzed by qPCR analysis. β-Actin is used as internal control.**(D-E)** The levels of SIRT1, PGC-1α, Nrf1, and Nrf2 in H9c2 and PC12 cells pretreated with different concentrations of GS for 48 h were examined by Western blot analysis. β-Actin is loading control. Semi-quantitative analysis of relative expression for each protein is shown on the right. Ctrl: control group. $^{*}P < 0.05$, $^{**}P < 0.01$, and $^{***}P < 0.001$*versus* Ctrl group.

Figure 5

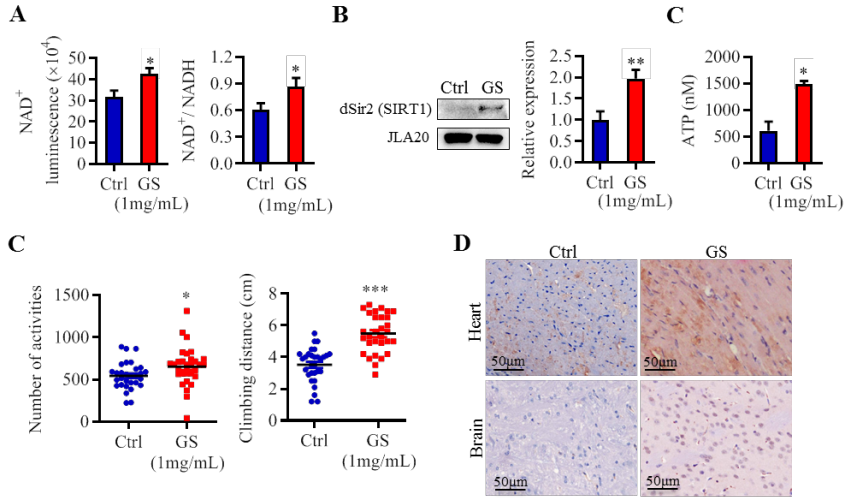

Fig. 5. GS increase NAD^+-dependent activation of SIRT1 in drosophila and mice. **(A)** The NAD^+level and NAD^+/NADH ratio in the brain tissue of 10 flies from control and GS treatment groups were analyzed by a bioluminescent detection kit. **(B)** The dSir2 (SIRT1) level in the drosophila brain of control and GS groups was detected by Western blot and quantified as the relative expression on the right. JLA20 is the loading control. **(C)** The activities and climbing distance of 30 flies per group were investigated after treatment with GS at 1 mg/mL for 7 d. **(D)** IHC staining of SIRT1 in the heart and brain tissues from control and GS-treated mice (10 mg/kg, 21 days) was performed. Scale bar=50 μm. Ctrl: control group. $^*P < 0.05$, $^{**}P < 0.01$, and $^{***}P < 0.001$ *versus* Ctrl group.

Figure 6

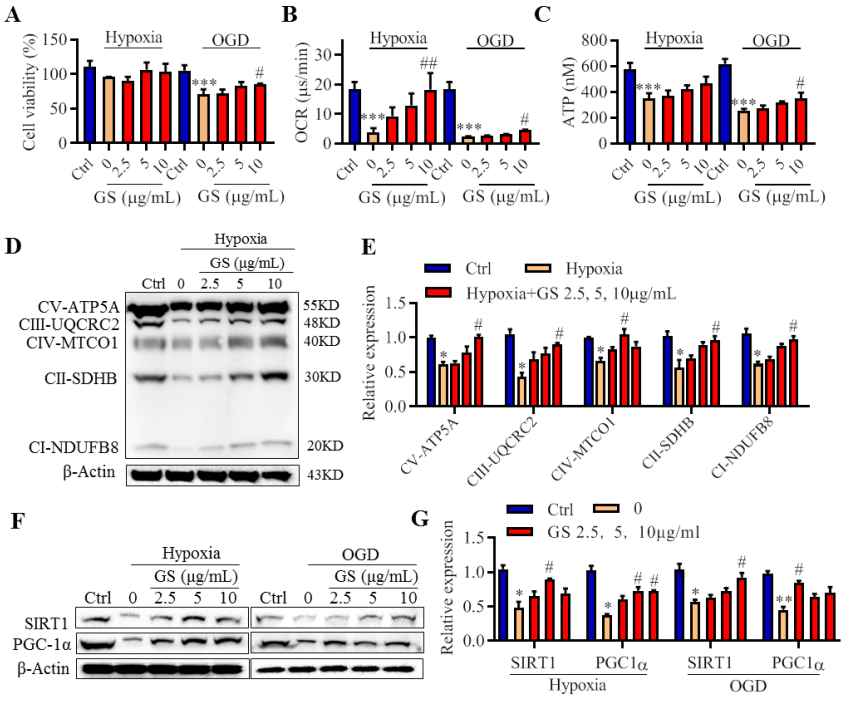

Fig. 6. GS increase mitochondrial function against the hypoxia- and OGD-induced injuries of the cardiomyocytes through the activation of SIRT1. **(A)** H9c2 cells were pretreated with GS for 48 h and kept in the medium with 800 μM $CoCl_2$ (hypoxia) or serum and glucose-free and 800 μM $CoCl_2$ (OGD) for 9 h. Cell viability was analyzed by the CCK8 assay kit and showed as the percentages. **(B-C)** Basal OCR and ATP content were measured in H9c2 cells, after GS pretreatment for 48 h and hypoxia/OGD incubation for 9 h. **(D)** H9c2 cells treated with GS for 48 h and incubated with hypoxia exposure for 9 h were collected and lysed to analyze the levels of complex I-V by Western blot. **(E)** Relative levels of CV-ATP5A, CIII-UQCRC2, CIV-MTCO1, CII-SDHB, and CI-NDUFB8 from (D) were calculated by Image J. **(F)** After GS treatment for 48 h, the expressions of SIRT1 and PGC-1α in H9c2 cells subjected to hypoxia and OGD injury were examined by Western blot. **(G)** Bar graphs show relative levels of SIRT1 and PGC-1α from (F). β-Actin is loading control. Ctrl: control group, $CoCl_2$: cobalt chloride. $^{*}P < 0.05$, $^{**}P < 0.01$, and $^{***}P < 0.001$ *versus* Ctrl group; $^{\#}P < 0.05$ and $^{\#\#}P < 0.01$ *versus* hypoxia or OGD group.

Figure 7

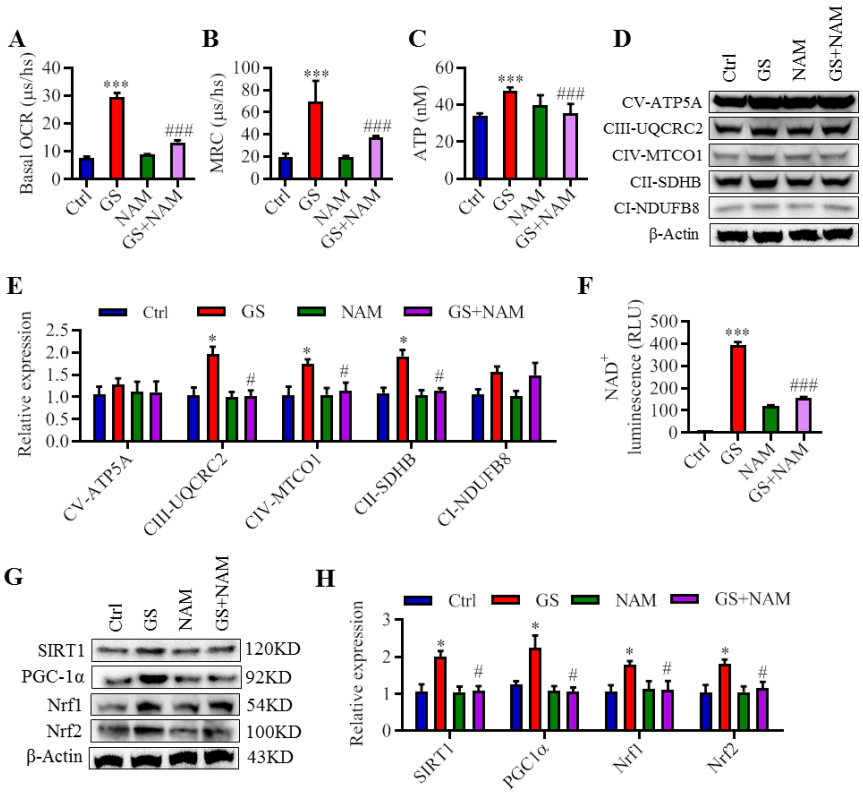

Fig. 7. The effect of GS on mitochondrial function was abrogated by NAM, a SIRT1 inhibitor. **(A-B)** Basal OCR and MRC in H9c2 cells were measured, after the treatment by GS and/or NAM for 48 h.**(C)** H9c2 cells were treated with GS and/or NAM for 48 h to measure ATP level by a bioluminescence detection kit. **(D)** The expressions of CV-ATP5A, CIII-UQCRC2, CIV-MTCO1, CII-SDHB, and CI-NDUFB8 in H9c2 cells treated with GS and/or NAM for 48 h were detected by Western blot. **(E)** Relative levels of five mitochondrial complexes from (D) are shown, after the quantification by ImageJ.**(F)** The effect of GS combined with NAM on the NAD^{+} level was analyzed by a NAD/NADH-Glo assay kit.**(G-H)** Total proteins of H9c2 cells treated with GS and/or NAM for 48 h were prepared and followed by Western blot analysis using antibodies against SIRT1, PGC1α, Nrf1, Nrf1, and β-Actin. Relative expression of these proteins was quantified with ImageJ and shown on the right. β-Actin is loading control. Ctrl: control group, OCR: oxygen

consumption rate, MRC: maximal respiration capacity. $^{*}P < 0.05$ and $^{***}P < 0.001$ *versus* Ctrl group; $^{\#}P < 0.05$ and $^{\#\#}P < 0.01$ *versus* GS+NAM group.

Figure 8

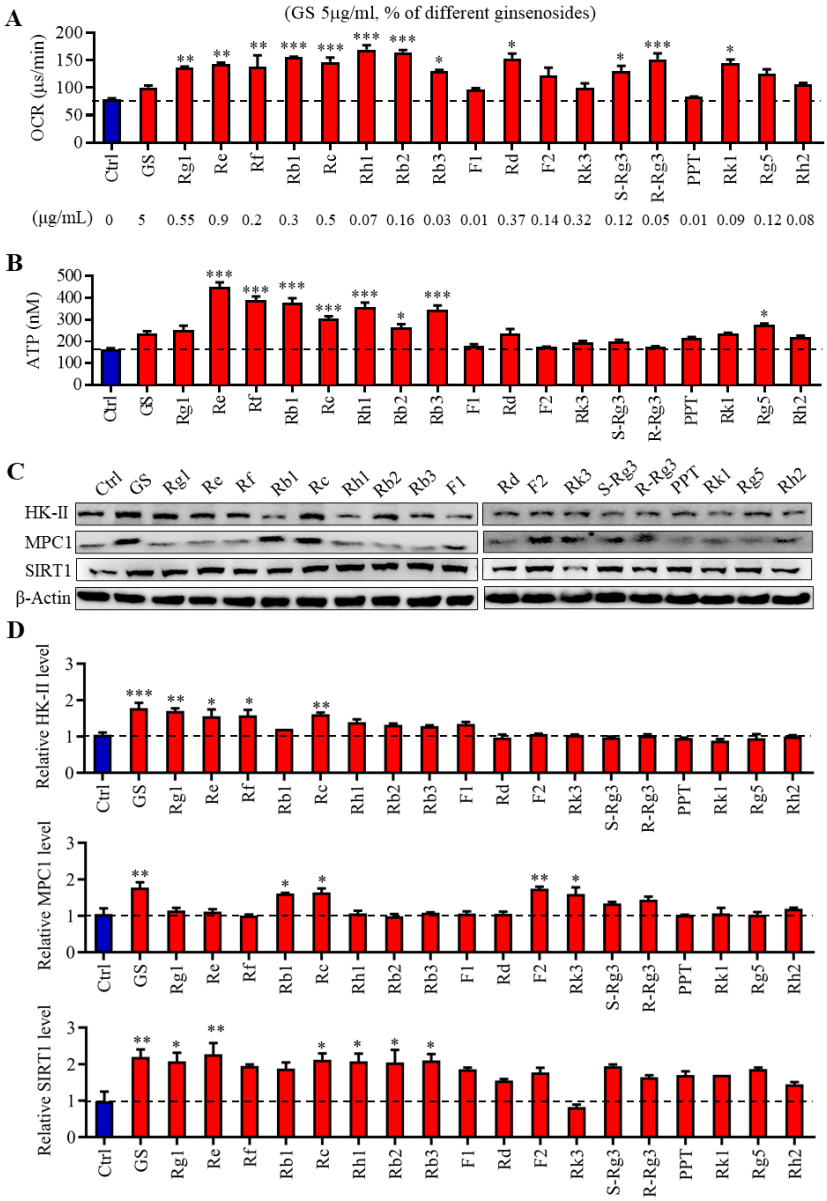

Fig. 8. The effects of main ginsenosides monomers on SIRT1-mediated mitochondrial function in H9c2 cells. **(A-B)**Basal OCR and ATP production were detected in H9c2 cells treated with GS or different ginsenoside monomer for 48 h as described in Materials and Methods. **(C-D)** After the pretreatment with different ginsenosides monomers at the composition percentage of GS (5μg/mL) for 48 h, the levels of HK-II, MPC1 and SIRT1 in H9c2 cells were detected by Western blot. Relative HK-II, MPC1, and SIRT1 expressions were quantified after the normalization to β-Actin. β-Actin is the loading control for Western blot analysis. Ctrl: control group, OCR: oxygen consumption rate. HK-II: Hexokinase-II, MPC1: mitochondrial pyruvate

carrier 1. $^{*}P < 0.05$, $^{**}P < 0.01$, and $^{***}P < 0.001$ *versus* Ctrl group.

Figure 9

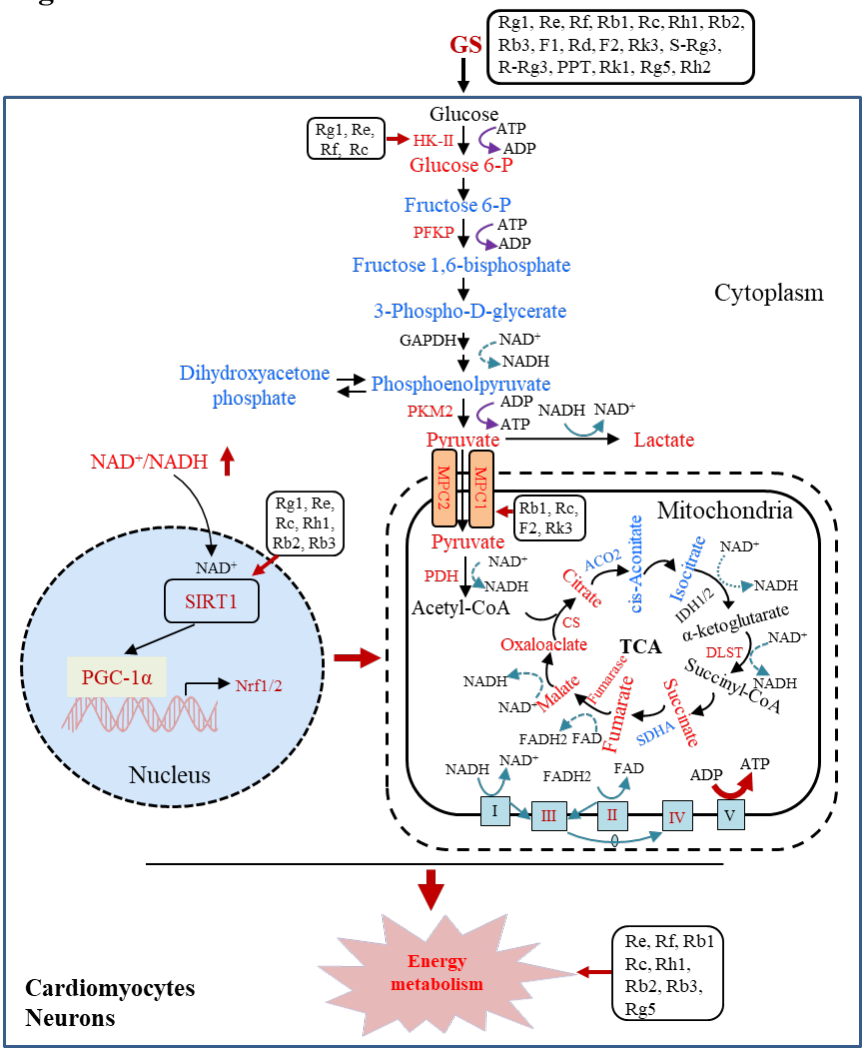

Fig. 9. Scheme indicating the molecular mechanism of total ginsenosides from Panax ginseng for promoting aerobic cell respiration and SIRT1 mitochondrial biosynthesis in cardiomyocytes and neurons. GS can increase the level of key metabolic enzymes and mitochondrial protein complexes II-IV to enhance TCA cycle and oxidative phosphorylation. Meanwhile, GS can promote the NAD^{+}level and activate the SIRT1-PGC-1α pathway to increase mitochondrial biosynthesis. GS-induced increased level (Red) and decreased level (Blue).